

Colloquium: Gravitational Form Factors of the Proton

V. D. Burkert,¹ L. Elouadrhiri,¹ F. X. Girod,¹ C. Lorcé,² P. Schweitzer,³ and P. E. Shanahan⁴

¹*Thomas Jefferson National Accelerator Facility, Newport News, VA, USA*

²*CPHT, CNRS, École polytechnique, Institut Polytechnique de Paris, 91120 Palaiseau, France*

³*Department of Physics, University of Connecticut, Storrs, CT 06269, USA*

⁴*Center for Theoretical Physics, Massachusetts Institute of Technology, Cambridge, MA 02139, USA*

(Dated: January, 17 2023)

The physics of the gravitational form factors of the proton, and their understanding within quantum chromodynamics, has advanced significantly in the past two decades through both theory and experiment. This Colloquium provides an overview of this progress, highlights the physical insights unveiled by studies of gravitational form factors, and reviews their interpretation in terms of the mechanical properties of the proton.

CONTENTS

I. Introduction	0
A. Anomalous magnetic moment	0
B. The proton's finite size	0
C. Discovery of partons	1
D. Colored quarks and gluons, QCD, and confinement	1
E. Proton mass, spin and D -term	2
II. The energy-momentum tensor	2
A. Definition of the EMT operator	2
B. Trace anomaly	3
C. Definition of the proton GFFs	3
D. Decomposition of proton mass	3
E. Decomposition of proton spin	5
III. Measuring gravitational form factors	5
A. Deeply virtual Compton scattering (DVCS)	5
B. DVCS with positron and electron beams	7
C. $\gamma\gamma^* \rightarrow \pi^0\pi^0$ and J/Ψ threshold production	7
D. Time-like Compton scattering, double DVCS and deeply virtual meson production	7
IV. Experimental results	8
A. DVCS in fixed-target and collider experiments	8
B. First extraction of the proton GFF $D_q(t)$	9
C. Future experimental developments to access GFFs.	11
D. Other phenomenological studies	12
V. Theoretical Results	12
A. Chiral symmetry and the D -term of the pion	12
B. GFFs in model studies	12
C. Limits in QCD and dispersion relations	13
D. Lattice QCD	14
VI. Interpretation	16
A. The static EMT	16
B. The stress tensor and the D -term	16
C. Normal forces and the sign of the D -term	17
D. The mechanical radius of the proton and neutron	17
E. First visualization of forces from experiment	17
F. The D -term and long-range forces	18
VII. Summary and outlook	19
Acknowledgments	20
Acronyms	20
References	21

I. INTRODUCTION

This Colloquium reviews the recent theoretical and experimental progress in studies of the gravitational form factors of the proton and other hadrons, which has shed fascinating new lights on the proton's structure and its mechanical properties. To place this emerging area in context, the history of proton structure and its description in quantum chromodynamics are first reviewed.

A. Anomalous magnetic moment

Soon after the proton (Rutherford, 1919) and neutron (Chadwick, 1932) were established as the constituents of atomic nuclei, experiments showed that these spin- $\frac{1}{2}$ particles with nearly equal masses $m_p \simeq m_n \simeq 940 \text{ MeV}/c^2$ are not pointlike elementary fermions. If they were, the Dirac equation would predict the magnetic moment of the proton to be one nuclear magneton $\mu_N \equiv e\hbar/(2m_p)$ and that of an electrically neutral particle like the neutron to be zero. Instead, the proton magnetic moment was measured to be about $\mu_p \simeq 2.5 \mu_N$ (Frisch and Stern, 1933). Later the neutron magnetic moment was found to be $\mu_n \simeq -1.5 \mu_N$ (Alvarez and Bloch, 1940); for the modern values of the magnetic moments see (Workman et al., 2022a). These experiments have shown that the nucleon is not a pointlike elementary particle, giving birth in 1933 to the field of proton structure.

Protons and neutrons are hadrons, particles that feel the strong force, which is the strongest interaction known in nature. Based on approximate isospin symmetry, they are understood as partnered (isospin up/down) states, referred to collectively as the nucleon (Heisenberg, 1932). As the constituents of nuclei, nucleons are responsible for more than 99.9% of the mass of matter in the visible universe, and have naturally become the most experimentally studied objects in hadronic physics.

B. The proton's finite size

An important milestone in the field of nucleon structure was brought by studies of elastic electron-proton

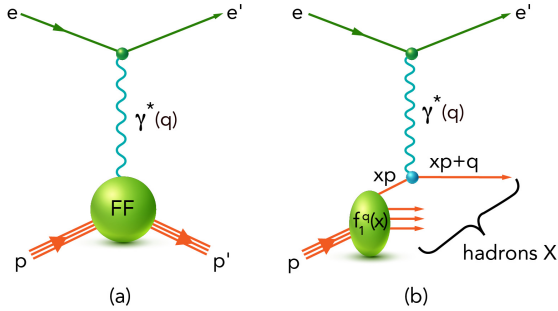


FIG. 1 (a) The elastic electron-proton scattering process in which the electromagnetic form factors (FFs) are measured. (b) Inclusive deep inelastic scattering (DIS) where the proton is dissociated into a final state consisting of unresolved hadrons. In the Bjorken limit $p \cdot q \rightarrow \infty$ and $Q^2 = -q^2 \rightarrow \infty$ with $x_B = Q^2/(2p \cdot q)$ fixed, DIS is interpreted in the so-called infinite-momentum frame as the scattering of electrons off point-like quarks carrying the fraction x of nucleon's momentum, where $x = x_B$ up to corrections suppressed by M_N^2/Q^2 .

scattering, shown in Fig. 1a, which revealed early insights into the proton's size. The deviations in scattering data from expectations for point-like particles are encoded in terms of form factors (FFs) defined through matrix elements of the electromagnetic current operator, $\langle p', \vec{s}' | J_{em}^\mu | p, \vec{s} \rangle$, where $|p, \vec{s}\rangle$ is the initial state of the proton with momentum p polarized along the \vec{s} direction, and analogously for the final proton state.

These FFs would be constants for pointlike particles, but they were found to be pronounced functions of the Mandelstam variable $t = (p' - p)^2$. A spin- $\frac{1}{2}$ particle has two electromagnetic FFs, $F_1(t)$ and $F_2(t)$, defined such that $F_1(0)$ is the electric charge in units of e , and $F_2(0)$ is the anomalous magnetic moment, i.e., the deviation from the value predicted by the Dirac equation, in units of μ_N . Knowledge of the t -dependence of electromagnetic FFs allowed information about the spatial distributions of electric charge and magnetization to be inferred (Sachs, 1962) (more discussion of this interpretation is given below). This led to the first determination of the proton charge radius of (0.74 ± 0.24) fm (McAllister and Hofstadter, 1956). These experiments have continued to this day, and using a variety of experimental techniques, they resulted in a much more precise knowledge of the proton's charge radius (Workman et al., 2022b).

C. Discovery of partons

The 1950s witnessed immense progress in accelerator and detection techniques followed by a proliferation of discoveries of strongly interacting particles and resonances, including particles like the antiproton, Δ , and Ξ , see the early review (Snow and M. M. Shapiro, 1961).

On the theory side, this led to the development of the quark model (Gell-Mann, 1964; Zweig, 1964) in which hadrons are classified according to quantum numbers which are understood to arise from various combinations of “quarks”. The “quarks” in this model were group-theoretical objects, and their dynamics were unknown.

The next milestone was brought by high-energy experiments carried out at the Stanford Linear Accelerator, where the Bjorken scaling predicted on the basis of current algebra and dispersion relation techniques (Bjorken, 1969) was observed in inclusive deep inelastic scattering (DIS) (Bloom et al., 1969). The response of the nucleon in DIS is described by structure functions which, on general grounds, are functions of the Lorentz invariants $p \cdot q$ and $Q^2 = -q^2$, where p^μ is the nucleon four-momentum and q^μ the four-momentum transfer, see Fig. 1b. Bjorken scaling is the property that, in the high-energy limit $p \cdot q \rightarrow \infty$ and $Q^2 \rightarrow \infty$ with their ratio fixed, the structure functions are, to a first approximation, functions of a single variable $x_B = Q^2/(2p \cdot q)$ which on kinematical grounds satisfies $0 < x_B < 1$.

The physical significance of this non-trivial observation was interpreted in the parton model (Feynman, 1969), where DIS process proceeds as shown in Fig. 1b, namely the electrons scatter off nearly free electrically-charged pointlike particles called partons, with a cross-section that can be calculated in quantum electrodynamics (QED). The structure of the nucleon in DIS is described in terms of parton distribution functions (PDFs), depicted by the green ellipse in Fig. 1b. In modern terminology, the PDFs in unpolarized DIS are denoted $f_1^a(x)$, with a labelling the type of parton. More precisely, $f_1^a(x) dx$ is the probability to find a parton of type a in the initial state inside of a nucleon moving with nearly the speed of light (an appropriate picture in DIS where $x \approx x_B$) and carrying a fraction of the nucleon momentum in the interval $[x, x + dx]$. It was soon realized that the electrically charged partons, identified with quarks and antiquarks, carry only half of the nucleon momentum between them.

D. Colored quarks and gluons, QCD, and confinement

The discovery of proton substructure and development of the parton model were key to establishing quantum chromodynamics (QCD) as the theory of the fundamental interaction between quarks carrying $N_c = 3$ different color charges (and antiquarks carrying the corresponding anticharges) (Gross and Wilczek, 1973; Politzer, 1973). The color forces are mediated by the exchange of spin-1 gluons which carry also color charges (as opposed to electrically neutral photons which mediate interactions in QED). Evidence for the existence of gluons has been found in the study of e^+e^- annihilation processes (Brandelik et al., 1980). Being electrically neutral, the gluons

are “invisible” in interactions with electrons, and account for the missing half of the proton momentum in DIS.

The QCD Lagrangian is given by

$$\mathcal{L} = \sum_q \bar{\psi}_q (i\not{D} + m_q)\psi_q - \frac{1}{4} F^2, \quad (1)$$

where $\bar{\psi}_q$ and ψ_q denote the quark and antiquark fields and m_q denotes the current quark masses. The summation runs over the quark flavors $q \in \{u, d, s, c, b, t\}$. The covariant derivative is defined as $iD_\mu = i\partial_\mu + gT^a A_\mu^a$ and $F^2 = F_{\mu\nu}^a F^{a\mu\nu}$ with $F_{\mu\nu}^a = \partial_\mu A_\nu^a - \partial_\nu A_\mu^a + gf^{abc} A_\mu^b A_\nu^c$, where T^a are the generators in the fundamental representation of $SU(N_c)$ with $a \in \{1, \dots, N_c^2 - 1\}$ and f^{abc} are the structure constants of the $SU(N_c)$ group. Non-abelian gauge theories like QCD are renormalizable ('t Hooft and Veltman, 1972) with the coupling constant $\alpha_s(\mu) = g(\mu)^2/(4\pi)$ depending on the renormalization scale μ . When it comes to describing hadrons, whose intrinsic scale sets $\mu \sim 1$ GeV, the interaction turns out to be strong because $\alpha_s(\mu)$ is large, and the solution of (1) requires nonperturbative techniques. However, in high-energy processes such as DIS, where the renormalization scale is identified with the hard scale of the process, $\alpha_s(Q)$ decreases with increasing Q (a property known as asymptotic freedom) explaining why quarks, antiquarks and gluons appear in such reactions as nearly free partons to a first approximation. The fact that free color charges are never observed in nature gave rise to the confinement hypothesis, whose theoretical explanation is still an outstanding open question.

E. Proton mass, spin and D -term

While the fundamental degrees of freedom and their interaction described in terms of the Lagrangian (1) are well-established, many questions remain open. For instance, in a “static” quark model one would naively attribute the spin $\frac{1}{2}$ of the nucleon to the spins of the quarks. In nature, due to the relatively light u - and d -quarks being confined within distances of $\mathcal{O}(1 \text{ fm})$, Heisenberg’s uncertainty principle implies an ultra-relativistic motion of the quarks. It must be expected that, e.g., the orbital motion of quarks has an important role in the spin budget of the nucleon. At the quantitative level, the nucleon spin decomposition is, however, still not known precisely (Ji et al., 2021). Another interesting open question is how 3 quarks with masses of 2-5 MeV/ c^2 can bind to give a nucleon mass of about 940 MeV/ c^2 . In other words, the mass of the visible universe comes essentially from QCD and has little to do with the Higgs mechanism.

The answers to these questions are described in the matrix elements of the energy-momentum tensor (EMT), an operator in quantum field theory of central importance that is associated with the invariance of the theory under

spacetime translations. These matrix elements encode key information including the mass and spin of a particle, the less well-known but equally fundamental D -term, as well as information about the distributions of energy, angular momentum, and various mechanical properties such as, e.g., internal forces inside the particle.

Since the gravitational interaction between a proton and an electron is (at currently achievable lab energies) 10^{-39} times weaker than their electromagnetic interaction, direct use of gravity to probe proton structure is impossible in electron-proton scattering, and in fact in any accelerator experiment in foreseeable future. Fortunately, indirect methods exist to acquire information about the EMT through studies of hard exclusive reactions. The purpose of this Colloquium is to review the progress in theory, experiment and interpretation of the EMT matrix elements.

II. THE ENERGY-MOMENTUM TENSOR

In this section, after reviewing the definition and properties of the EMT in QCD, the gravitational form factors (GFFs) of the proton are introduced. It is shown how GFFs can be leveraged to elucidate the proton’s mass and spin decompositions.

A. Definition of the EMT operator

In QCD, the EMT $T^{\mu\nu} = \sum_q T_q^{\mu\nu} + T_G^{\mu\nu}$ can be decomposed into gauge-invariant quark and gluon parts as

$$\begin{aligned} T_q^{\mu\nu} &= \bar{\psi}_q \gamma^\mu iD^\nu \psi_q, \\ T_G^{\mu\nu} &= -F^{a\mu\lambda} F_{\lambda}^{a\nu} + \frac{1}{4} g^{\mu\nu} F^2 \end{aligned} \quad (2)$$

with $g_{\mu\nu} = \text{diag}(+1, -1, -1, -1)$ the Minkowski metric. In quantum field theory, the expressions for the matrix elements of bare operators contain divergences and must be renormalized ('t Hooft and Veltman, 1972). Therefore, each term in (2) is understood as a renormalized operator defined at some renormalization scale μ . The components of the EMT are interpreted in the same way as in the classical theory, namely T^{00} is the energy density, T^{0i} is the momentum density, T^{i0} is the energy flux, and T^{ij} is the momentum flux or stress tensor. In the literature, one often considers only the symmetric part of (2), known as the Belinfante EMT (Belinfante, 1962). The antisymmetric part is a total derivative whose presence does not affect the conserved Poincaré charges (i.e. four-momentum and spin) but impacts the definition of the corresponding densities (Leader and Lorcé, 2014; Lorcé et al., 2018).

B. Trace anomaly

At the classical level, the QCD Lagrangian (1) is approximately invariant under scale transformations $x \mapsto x' = \lambda x$. More precisely, the associated classical (dilation) current is conserved up to quark mass effects, which are small for u - and d -flavors. Contrary to spacetime translations, this symmetry is affected by quantum corrections. As a result, even though the renormalized EMT looks formally the same as in the classical theory, its trace (which measures the non-conservation of the dilation current) receives anomalous contributions (Collins et al., 1977; Nielsen, 1977)

$$g_{\mu\nu}T^{\mu\nu} = \sum_q (1 + \gamma_m) m_q \bar{\psi}_q \psi_q + \frac{\beta(g)}{2g} F^2, \quad (3)$$

where γ_m is the anomalous quark mass dimension and $\beta(g) = \partial g / \partial \ln \mu$ is the QCD beta function. As will be discussed later, this trace anomaly plays an important role when discussing the mass and mechanical properties of the proton. Note that $g_{\mu\nu}T_q^{\mu\nu}$ and $g_{\mu\nu}T_G^{\mu\nu}$ mix with each other under renormalization, and each one contains both quark and gluon scalar operators (Ahmed et al., 2022; Hatta et al., 2018; Tanaka, 2019).

C. Definition of the proton GFFs

The gateway to the mass and spin decompositions, and mechanical properties of the proton, are the matrix elements of the EMT operator. In terms of proton momentum eigenstates $|p, \vec{s}\rangle$, polarized in the \vec{s} direction and normalized as $\langle p', \vec{s}' | p, \vec{s} \rangle = 2p^0 (2\pi)^3 \delta^{(3)}(\vec{p}' - \vec{p})$, the EMT matrix elements can conveniently be parametrized as (Bakker et al., 2004; Ji, 1997b; Kobzarev and Okun, 1962; Lorcé et al., 2022b; Pagels, 1966)

$$\begin{aligned} \langle p', \vec{s}' | T_a^{\mu\nu}(0) | p, \vec{s} \rangle &= \bar{u}(p', \vec{s}') \left[A_a(t) \frac{P^\mu P^\nu}{M_N} \right. \\ &+ D_a(t) \frac{\Delta^\mu \Delta^\nu - g^{\mu\nu} \Delta^2}{4M_N} + \bar{C}_a(t) M_N g^{\mu\nu} \\ &\left. + J_a(t) \frac{P^{\{\mu} i \sigma^{\nu\} \lambda} \Delta_\lambda}{M_N} - S_a(t) \frac{P^{[\mu} i \sigma^{\nu] \lambda} \Delta_\lambda}{M_N} \right] u(p, \vec{s}) \end{aligned} \quad (4)$$

for $a \in \{q, G\}$. Here $u(p, \vec{s})$ is the usual free Dirac spinor, M_N denotes the nucleon mass, and the symmetric kinematical variables are defined as

$$P = \frac{1}{2}(p' + p), \quad \Delta = p' - p, \quad t = \Delta^2. \quad (5)$$

The first four GFFs are associated with the symmetric (Belinfante) part of the EMT $T_a^{\{\mu\nu\}} \equiv \frac{1}{2}(T_a^{\mu\nu} + T_a^{\nu\mu})$. As one can see from (2), only the quark part receives an antisymmetric contribution $T_q^{[\mu\nu]} \equiv \frac{1}{2}(T_q^{\mu\nu} - T_q^{\nu\mu})$ and

$S_G(t) = 0$. The GFFs of specific partons inherit a renormalization scale dependence from the associated operators, which is omitted in the notation for convenience. The total GFFs (summed over q and G) of the symmetric EMT are renormalization scale independent.

On top of restricting the number of GFFs, Poincaré symmetry imposes additional constraints, namely

$$A(0) = \sum_q A_q(0) + A_G(0) = 1, \quad (6)$$

$$J(0) = \sum_q J_q(0) + J_G(0) = \frac{1}{2}, \quad (7)$$

$$\frac{1}{2} \Delta \Sigma = \sum_q S_q(0), \quad (8)$$

$$\bar{C}(t) = \sum_q \bar{C}_q(t) + \bar{C}_G(t) = 0, \quad (9)$$

where (6) follows from translation symmetry (Ji, 1998), while (7) and (8) result from Lorentz symmetry (Bakker et al., 2004; Ji, 1997b), with $\frac{1}{2} \Delta \Sigma$ denoting the quark spin contribution to the nucleon spin. The constraint (9), valid for any t , follows from EMT conservation $\partial_\mu T^{\mu\nu} = 0$. Interestingly, the renormalization-scale invariant quantity (Polyakov and Weiss, 1999)

$$D \equiv D(0) = \sum_q D_q(0) + D_G(0), \quad (10)$$

known as the \bar{D} -term (D stands for the German word *Druck* meaning pressure), is a global property of the proton (and, in fact, any hadron), whose value is not fixed by spacetime symmetries (Polyakov and Weiss, 1999). Its physical interpretation will be discussed in Sec. VI.

Until recently, the only information about GFFs known from phenomenology was $A_a(0) = \int_{-1}^1 dx x f_1^a(x)$, corresponding to the fraction of proton momentum carried by the partons a as inferred from DIS experiments, and $S_q(0) = \frac{1}{2} \int_{-1}^1 dx g_1^q(x)$, where $g_1^q(x)$ is the quark helicity distribution (Aidala et al., 2013).

D. Decomposition of proton mass

As the GFFs encode matrix elements of the EMT, the values taken by the former at $t = 0$ provide the necessary quantitative input for decomposing the nucleon mass and spin into various quark and gluon contributions.

The concept of mass is directly related to the EMT. The starting point is the total four-momentum operator

$$\mathcal{P}^\mu = \int d^3r T^{0\mu}, \quad (11)$$

defined in terms of the total EMT of the system. The corresponding expectation value in a four-momentum eigenstate can be expressed as

$$\langle \mathcal{P}^\mu \rangle \equiv \frac{\langle p, \vec{s} | \mathcal{P}^\mu | p, \vec{s} \rangle}{\langle p, \vec{s} | p, \vec{s} \rangle} = p^\mu, \quad (12)$$

which is just the forward (i.e. $\Delta = 0$) matrix element with appropriate normalization. Using translation symmetry $T^{\mu\nu}(x) = e^{iP \cdot x} T^{\mu\nu}(0) e^{-iP \cdot x}$, one finds that (12) can be put into the form

$$\frac{\langle p, \vec{s} | T^{0\mu}(0) | p, \vec{s} \rangle}{2p^0} = p^\mu. \quad (13)$$

A mass decomposition arises naturally from (13) by considering the energy component $\mu = 0$ in the rest frame (or equivalently by contraction with the four-velocity p^μ/M_N in an arbitrary frame). One then finds that the quark and gluon contributions to the proton mass $M_N = \sum_q U_q + U_G$ (Lorcé, 2018a) are given by

$$U_a = \frac{\langle p, \vec{s} | T_a^{00}(0) | p, \vec{s} \rangle}{2p^0} \Big|_{\vec{p}=\vec{0}} = [A_a(0) + \bar{C}_a(0)] M_N. \quad (14)$$

Combining this with the definition of the quark mass contribution

$$U_m = \sum_q \sigma_q \equiv \frac{\langle p, \vec{s} | \sum_q m_q \bar{\psi}_q \psi_q | p, \vec{s} \rangle}{2p^0} \Big|_{\vec{p}=\vec{0}}, \quad (15)$$

one obtains a three-term mass decomposition (Metz et al., 2020; Rodini et al., 2020)

$$M_N = \sum_q U_q^{\text{kin+pot}} + U_m + U_G, \quad (16)$$

where $U_q^{\text{kin+pot}} \equiv U_q - \sigma_q$ is interpreted as the quark kinetic and potential energy.

More generally, one can consider the entire set of components

$$\frac{\langle p, \vec{s} | T_a^{\mu\nu}(0) | p, \vec{s} \rangle}{2p^0} \Big|_{\vec{p}=\vec{0}} = \begin{pmatrix} U_a & 0 & 0 & 0 \\ 0 & W_a & 0 & 0 \\ 0 & 0 & W_a & 0 \\ 0 & 0 & 0 & W_a \end{pmatrix}, \quad (17)$$

where $W_a = -\bar{C}_a(0)M_N$ is the pressure-volume work defined as the partial isotropic stress $\frac{1}{3} \sum_i \langle T_a^{ii} \rangle$ considered in the proton rest frame and integrated over all space. For a massive bound system in mechanical equilibrium, the total pressure-volume work should vanish (Laue, 1911)

$$\sum_a W_a = 0, \quad (18)$$

a result known as the virial theorem for a closed system (Lorcé et al., 2021). Since U_a and W_a mix under Lorentz transformations, two distinct constraints $A(0) = 1$ and $\bar{C}(0) = 0$ can then be derived from four-momentum conservation expressed by (13).

In addition to the mass decomposition (16) resulting directly from the definition of the proton mass as the rest-frame energy (usually expressed in the covariant way as $p^2 = M_N^2$), two other mass decompositions have been

proposed in the literature with the particularity of involving *both* U_a and W_a . The first follows from the trace of (17) and the virial theorem (18), leading to the expression (Hatta et al., 2018; Tanaka, 2019)

$$M_N = \sum_q I_q + I_G \quad (19)$$

with $I_a = U_a - 3W_a = [A_a(0) + 4\bar{C}_a(0)] M_N$. An older variant of this trace decomposition (Donoghue et al., 2014; Shifman et al., 1978) is given by the forward matrix element of (3)

$$M_N = M_m + M_A, \quad (20)$$

where $M_m = U_m$ and the anomalous contribution is

$$M_A = \frac{\langle p, \vec{s} | \sum_q \gamma_m m_q \bar{\psi}_q \psi_q + \frac{\beta(g)}{2g} F^2 | p, \vec{s} \rangle}{2p^0} \Big|_{\vec{p}=\vec{0}}. \quad (21)$$

The difference between (19) and (20) is related to the operator mixing mentioned earlier. The quantities $\sum_q I_q$ and I_G are scale-dependent and can be simply interpreted as the traces of the quark and gluon contributions to the EMT (each containing part of the trace anomaly), whereas M_m and M_A are scale-independent and are interpreted as the non-anomalous and anomalous contributions to the EMT trace. Current phenomenology (Hoferichter et al., 2016) and Lattice QCD calculations (Alexandrou et al., 2020b) indicate that $M_m/M_N \approx 10\%$, which is at the origin of the claim that most of the proton mass comes from the trace anomaly (and hence from the gluons, since γ_m is small). This picture based on (20) is, however, misleading as one has in fact decomposed $g_{\mu\nu} T^{\mu\nu} = T^{00} - \sum_i T^{ii}$ and therefore combined the internal energies U_a with the pressure-volume works W_a . Since $\sum_q U_q$ and U_G turn out to be of the same order of magnitude, the smallness of M_m (or $\sum_q I_q$) relative to M_A (or I_G) actually indicates that the quark (gluon) pressure-volume work is large and positive (negative) (Lorcé, 2018a).

The popular mass decomposition (Ji, 1995a,b, 2021) can be seen as a blend of (16) and (20). Instead of immediately splitting the EMT into quark and gluon contributions as in (2), one first separates it into traceless and pure trace tensors

$$T^{\mu\nu} = (T^{\mu\nu} - \frac{1}{4} g^{\mu\nu} g_{\alpha\beta} T^{\alpha\beta}) + \frac{1}{4} g^{\mu\nu} g_{\alpha\beta} T^{\alpha\beta}. \quad (22)$$

The motivation is that these tensors belong to different representations of the Lorentz group, and hence do not mix under Lorentz transformations or renormalization. Considering the rest-frame expectation value of the energy component $\mu = \nu = 0$, one concludes using the virial theorem (18) that 3/4 of the proton mass comes from the traceless part, and 1/4 comes from the pure trace part. As a second step, the pure trace part is decomposed similarly to (20), while the traceless part is decomposed into

quark and gluon contributions, similarly to (2). One then arrives at

$$M_N = \sum_q M_q + M_G + \frac{1}{4}(M_m + M_A) \quad (23)$$

with $M_a = \frac{3}{4}(U_a + W_a) = \frac{3}{4}A_a(0) M_N$ for $a = q, G$. As a final step, one rearranges the quark mass contribution

$$M_N = \sum_q M'_q + M_m + M_G + \frac{1}{4}M_A \quad (24)$$

with $M'_q \equiv M_q - \frac{3}{4}\sigma_q$, similarly to (16). A convenient feature of this four-term mass decomposition is that there is no need to determine the value of $\bar{C}_a(0)$, simplifying the scale dependence of the individual terms. Recalling that the values of the $A_a(0)$ are known from DIS, cf. Sec. II.C, the $M_{q,G}$ terms are directly proportional to measurable quantities. The drawback, however, is that the corresponding renormalized operators do not in general have a clean interpretation in terms of parton energies (Lorcé et al., 2021; Metz et al., 2020). Note also that only *two* independent inputs, viz. $\sum_q A_q(0)$ and $\sum_q \sigma_q$, are needed to fix the values of the four terms in (24). The latter are therefore not independent and satisfy the relation

$$\sum_q M'_q + M_G = \frac{3}{4}M_A, \quad (25)$$

which is a direct consequence of the virial theorem.

E. Decomposition of proton spin

A similar discussion elucidates the proton spin decomposition. The total angular momentum (AM) operator is defined, in terms of the Belinfante (symmetric) EMT $T_{\text{Bel}}^{\mu\nu} = T^{\{\mu\nu\}}$, as

$$\mathcal{J}^i = \int d^3r \epsilon^{ijk} r^j T_{\text{Bel}}^{0k}. \quad (26)$$

Because of the explicit factor of r^j , the forward matrix elements of this operator turn out to be ill-defined. A proper treatment requires the use of wave packets and amounts to considering matrix elements with non-vanishing momentum transfer (Bakker et al., 2004; Leader and Lorcé, 2014). The forward limit is then recovered at the end of the calculation as a consequence of the integration over all space.

For convenience, only the longitudinal AM (i.e. the component along the proton average momentum $\vec{P} = \frac{1}{2}(\vec{p}' + \vec{p})$ defining the z -direction) is considered here. The discussion about the transverse AM turns out to be much more complex because of its dependence on both $|\vec{P}|$ and the choice of origin, see e.g. (Lorcé, 2018b, 2021) and references therein. From the splitting of the EMT in (2),

one finds that the quark and gluon contributions to the proton spin $\langle \mathcal{J}^z \rangle = \sum_q J_q^z + J_G^z$ are given by (Ji, 1997b)

$$J_a^z = J_a(0), \quad (27)$$

for a proton polarized in the z -direction.

Working instead with an asymmetric EMT, the quark AM operator can be further decomposed into orbital and intrinsic AM terms

$$\mathcal{J}_q^i = \int d^3r \epsilon^{ijk} r^j T_q^{0k} + \int d^3r \frac{1}{2} \bar{\psi}_q \gamma^i \gamma_5 \psi_q. \quad (28)$$

Calculating the corresponding matrix elements, one then finds that $J_q^z = L_q^z + S_q^z$ with

$$L_q^z = J_q(0) - S_q(0), \quad (29)$$

$$\sum_q S_q^z = \frac{1}{2} \Delta \Sigma.$$

Combining the results (28) and (29) with the fact that the proton is a spin- $\frac{1}{2}$ particle, one arrives at the constraints given in (7) and (8).

Since gluons are spin-1 particles, one may wonder whether the gluon AM could also be decomposed into orbital and intrinsic contributions. This can be done, but it requires non-local operators to preserve gauge invariance (Chen et al., 2008; Hatta, 2012; Leader and Lorcé, 2014; Lorcé, 2013a,b; Wakamatsu, 2014). One is then led to the canonical (or Jaffe-Manohar) spin decomposition (Jaffe and Manohar, 1990), to be distinguished from the one derived here from the local EMT (2) and known as the kinetic (or Ji) spin decomposition (Ji, 1997b).

III. MEASURING GRAVITATIONAL FORM FACTORS

There is no direct way to measure the proton GFFs, as it would require measurements of the graviton-proton interaction (Kobzarev and Okun, 1962; Pagels, 1966). More recent theoretical developments have shown, however, that the GFFs may be probed indirectly in various exclusive processes. This is the subject of this section.

A. Deeply virtual Compton scattering (DVCS)

In DVCS, the most explored process so far that accesses the GFFs, high-energy charged leptons scatter off protons or nuclei by exchanging a deeply virtual photon, producing a real photon in the final state (Ji, 1997a; Müller et al., 1994; Radyushkin, 1996). In the limit $Q^2 \rightarrow \infty$ and $P \cdot q \rightarrow \infty$ with $(-t) \ll Q^2$, the process is described in QCD with collinear factorization (Collins and Freund, 1999). In this limit the DVCS amplitude is written in terms of a “hard part” which can be calculated order by order in perturbative QCD, and a nonperturbative “soft part” described in terms of generalized parton

distributions (GPDs) as shown in Fig. 2a. GPDs are universal, i.e., the same non-perturbative functions enter the description of different hard exclusive reactions.

GPDs are functions of x , ξ , t , where the skewness variable ξ , given in the high-energy limit by $\xi = x_B/(2-x_B)$, and t are observable, while x enters the description of the DVCS amplitude only as an integration variable and is integrated over in DVCS observables. GPDs encompass both PDFs and the electromagnetic FFs discussed in Sec. I. Starting from GPDs, one recovers PDFs when $\xi \rightarrow 0$ and $t \rightarrow 0$; integrating particular GPDs over x yields the electromagnetic FFs.

GPDs parameterize the matrix elements of certain non-local operators which can be expanded in terms of an infinite tower of local operators with various J^{PC} quantum numbers. This includes operators with the quantum numbers of the graviton ($J = 2$), and so part of the information about how the proton would interact with a graviton is encoded within this tower. As the electromagnetic coupling to quarks is many orders of magnitude stronger than gravity, the DVCS process is an effective tool to probe the proton's gravitational properties. Gluon GPDs are accessible in DVCS only at higher orders in α_s .

The leading contribution to DVCS is described in terms of four GPDs. Two of them, namely $H_q(x, \xi, t)$ and $E_q(x, \xi, t)$, give access to quark GFFs as follows

$$\begin{aligned} \int_{-1}^1 dx x H_q(x, \xi, t) &= A_q(t) + \xi^2 D_q(t), \\ \int_{-1}^1 dx x E_q(x, \xi, t) &= B_q(t) - \xi^2 D_q(t), \end{aligned} \quad (30)$$

where $B_q(t) = 2J_q(t) - A_q(t)$. $B_q(0)$ is the quark contribution to the proton's anomalous gravitomagnetic moment. Analogous relations hold for gluons, and $B(0) = \sum_a B_a(0)$ vanishes (Brodsky et al., 2001; Cotogno et al., 2019; Kobzarev and Okun, 1962; Lorcé and Lowdon, 2020; Lowdon et al., 2017; Teryaev, 1999) due to the constraints (6) and (7).

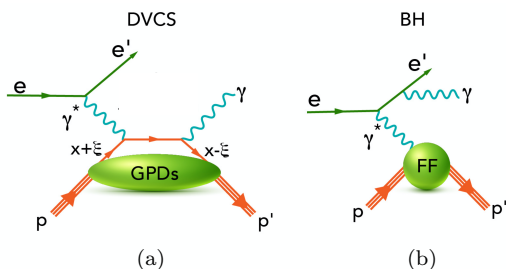


FIG. 2 (a) QCD factorization of the DVCS amplitude. The perturbatively calculable “hard part” is shown to lowest order in the strong coupling. The nonperturbative “soft part” is described by the universal quark GPDs. (b) One of the QED diagrams for the amplitude of the Bethe-Heitler process, which has the same final state as DVCS and interferes with it. The Bethe-Heitler process is calculable requiring only the proton electromagnetic FFs as input.

The actual observables in DVCS are Compton form factors (CFFs), e.g. $\mathcal{H}(\xi, t)$, which are complex-valued convolution integrals defined at leading order in $\alpha_s(Q)$

$$\begin{aligned} \text{Re}\mathcal{H}(\xi, t) + i \text{Im}\mathcal{H}(\xi, t) = \\ \sum_q e_q^2 \int_{-1}^1 dx \left[\frac{1}{\xi - x - i\epsilon} - \frac{1}{\xi + x - i\epsilon} \right] H_q(x, \xi, t). \end{aligned} \quad (31)$$

and similarly for other GPDs. The CFFs can be related to experimentally accessible quantities such as differential cross sections and beam and target polarization asymmetries.

The DVCS cross section is typically very small. Fortunately, DVCS interferes with the Bethe-Heitler process, which can be computed in QED given the proton's electromagnetic FFs, and has the same final state but with the final state photon emitted from the electron lines, see Fig. 2b. The interference term projects out $\text{Im}\mathcal{H}(\xi, t)$ when a spin-polarized electron beam is employed, while $\text{Re}\mathcal{H}(\xi, t)$ contributes dominantly to the unpolarized DVCS cross section, and may be constrained through precise unpolarized cross section measurements.

The convolution integrals like (31) cannot be inverted in a model-independent way to yield GPDs (Bertone et al., 2021). However, with experimental information from other exclusive processes becoming available (to be discussed below), the GPDs may be further constrained. Presently, a model-independent extraction of the GPDs and, via (30), of the GFFs $A_q(t)$ and $J_q(t)$ is not possible. In the case of the GFF $D_q(t)$, however, the situation is more fortunate. In particular, the real and imaginary parts of $\mathcal{H}(\xi, t)$ are related by the fixed- t dispersion relation (Anikin and Teryaev, 2008; Diehl and Ivanov, 2007)

$$\begin{aligned} \text{Re}\mathcal{H}(\xi, t) &= \mathcal{C}_{\mathcal{H}}(t) \\ &+ \frac{1}{\pi} \text{P.V.} \int_0^1 d\xi' \left[\frac{1}{\xi - \xi'} - \frac{1}{\xi + \xi'} \right] \text{Im}\mathcal{H}(\xi', t), \end{aligned} \quad (32)$$

where P.V. denotes the principal value of the Cauchy integral. This expression contains a real subtraction term $\mathcal{C}_{\mathcal{H}}(t)$ given by

$$\mathcal{C}_{\mathcal{H}}(t) = 2 \sum_q e_q^2 \int_{-1}^1 dz \frac{D_{\text{term}}^q(z, t)}{1 - z}, \quad (33)$$

where $D_{\text{term}}^q(z, t)$, originally introduced in (Polyakov and Weiss, 1999) and further elucidated in (Teryaev, 2001), has the expansion (Goeke et al., 2001)

$$D_{\text{term}}^q(z, t) = (1 - z^2) \sum_{\text{odd } n} d_n^q(t) C_n^{3/2}(z) \quad (34)$$

with $C_n^\alpha(z)$ the Gegenbauer polynomials which diagonalize the leading-order evolution equations (the renormalization scale dependence is suppressed throughout this

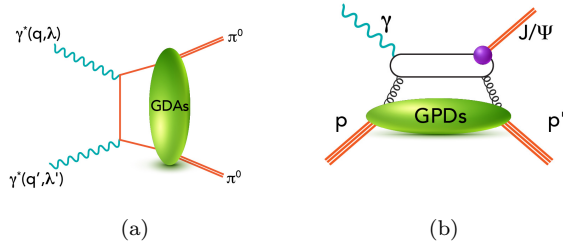


FIG. 3 (a) The process $\gamma\gamma^* \rightarrow \pi^0\pi^0$ is described in terms of generalized distribution amplitudes (GDAs), which provide access to GFFs in the time-like region $t > 0$. (b) Threshold J/Ψ photoproduction on proton. This process is sensitive to the gluon GPDs.

work). In the limit of renormalization scale $\mu \rightarrow \infty$, all $d_n^q(t)$ go to zero except $d_1^q(t)$, which is related to the GFF $D_q(t)$ as follows

$$D_q(t) = \frac{4}{5} d_1^q(t) = \int_{-1}^1 dz z D_{\text{term}}^q(z, t). \quad (35)$$

Thus, extracting information on $\text{Im}\mathcal{H}(\xi, t)$ and $\text{Re}\mathcal{H}(\xi, t)$ and their scale dependence from experimental data provides access to the GFF $D_q(t)$.

B. DVCS with positron and electron beams

When DVCS data with positron and electron beams are available, it is possible to measure the beam charge asymmetry $A_C = (\sigma_{\text{DVCS}}^e - \sigma_{\text{DVCS}}^{e^+}) / (\sigma_{\text{DVCS}}^e + \sigma_{\text{DVCS}}^{e^+})$. At leading twist, the numerator of A_C is given by the real part of the DVCS Bethe-Heitler interference term providing the cleanest access to $\text{Re}\mathcal{H}$ (Belitsky *et al.*, 2002; Kivel *et al.*, 2001). In contrast to this, in DVCS with electrons (or positrons) alone, additional theoretical assumptions in the CFF extraction procedure are unavoidable (Burkert *et al.*, 2021).

C. $\gamma\gamma^* \rightarrow \pi^0\pi^0$ and J/Ψ threshold production

The process $\gamma\gamma^* \rightarrow \pi^0\pi^0$ shown in Fig. 3a can be studied, e.g., at electron-positron colliders, and is described in terms of generalized distribution amplitudes which correspond to GPDs continued analytically from the t - to the s -channel (Diehl *et al.*, 1998; Müller *et al.*, 1994). In this way, one can access information on GFFs in the time-like region where $t > 0$. This process provides a unique opportunity to study the structure of unstable hadrons like pions that are not available as targets.

Exclusive J/Ψ photoproduction at threshold (Kharzeev, 1996, 2021), depicted in Fig. 3b, is expected to be sensitive to gluon GPDs, which in DVCS are accessible only at higher orders in α_s . The process of heavy vector quarkonium photoproduction was shown to factorize in the heavy quark limit at one-loop order

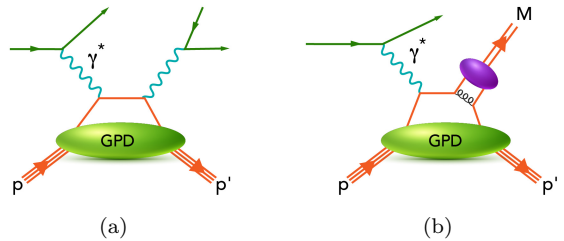


FIG. 4 The leading DDVCS diagram (a) and one of the leading diagrams for Deeply Virtual Meson Production (b). The ellipse where the meson is produced is the nonperturbative distribution amplitude.

in perturbative QCD (Ivanov *et al.*, 2004). While it was argued that the factorization in terms of gluon GPDs remains valid at threshold (Guo *et al.*, 2021), a recent study has challenged this picture (Sun *et al.*, 2021) and the theoretical status of this process is currently uncertain. J/Ψ photoproduction can also be studied with quasi-real photons of virtualities as low as $Q^2 \lesssim 0.1 \text{ GeV}^2$ emitted by electrons, in conjunction with electroproduction and DVCS. Both processes have been used to obtain information about GFFs, and will be discussed in more detail in Sec. IV.

D. Time-like Compton scattering, double DVCS and deeply virtual meson production

Several other processes provide complementary information about the nucleon GFFs. One of them is time-like Compton scattering (TCS), $\gamma p \rightarrow p' \gamma^*$, where the final state virtual photon produces an e^+e^- pair (Berger *et al.*, 2002; Chatagnon *et al.*, 2021; Pire *et al.*, 2011). This time-reversed version of DVCS provides an important opportunity to test the universality of GPDs. In TCS, $\text{Im}\mathcal{H}$ can be accessed through the polarized beam spin asymmetry and $\text{Re}\mathcal{H}$ through a forward-backward asymmetry of the final-state e^+e^- pair in its centre-of-mass frame.

The double DVCS (DDVCS) process displayed in Fig. 4a may play an important role at future facilities. It is a variant of DVCS with the final-state time-like photon decaying into a e^+e^- or $\mu^+\mu^-$ pair. While in DVCS the GPDs are sampled along the lines $x = \pm\xi$ in the convolution integrals (31), this constraint is relaxed in DDVCS due to the variable invariant mass of the lepton pair. This is an advantage of this process, and will be of importance for less model-dependent global extractions of GPDs.

Deeply virtual meson production is another process sensitive to GPDs, providing another important test of their universality, see Fig. 4b. Production of different vector mesons provides sensitivity to GPDs of different quark flavors which is an advantage over DVCS. At the same time, however, this process is more difficult to an-

alyze than DVCS since gluons contribute on the same footing as quarks (Fig. 4b only shows a quark diagram) and one in general expects larger power corrections.

Finally, a new class of hard scattering processes with a larger number of particles in the final state has recently emerged (Qiu and Yu, 2022). The $\gamma N \rightarrow \gamma\gamma N'$ process (Grocholski et al., 2022; Pedrak et al., 2020) with a large invariant diphoton mass is particularly interesting since, contrary to DVCS and TCS, it gives access to the charge-conjugation odd part of the quark GPDs. Other processes involving a meson-meson (Ivanov et al., 2002) or photon-meson pair (Boussarie et al., 2017; Duplancić et al., 2018) produced with a large invariant mass have also been proposed.

Sec. IV will focus on DVCS and TCS as the most suitable processes for near-future studies of proton CFFs.

IV. EXPERIMENTAL RESULTS

This section presents a brief overview of the current landscape of the experimental program targeting the probing of GPDs and the extraction of the GFFs of the nucleon and other hadrons. The first extraction of the proton D -term form factor $D_q(t)$ from experiment based on data from Jefferson Lab (JLab) is described in detail. The extraction of $D_q(t)$ of the neutral pion from Belle data, and other phenomenological results, are also reviewed.

A. DVCS in fixed-target and collider experiments

In this section, the past, current and planned DVCS experiments are briefly reviewed. Experimental measurements of DVCS are difficult as they require high luminosity to measure small cross sections with polarized electron, positron or muon beams at different energies, and employing polarized nucleon targets, both longitudinal and transverse, to measure observables with sensitivity to different combinations of CFFs. The measurements also require advanced detection capabilities to ensure reaction exclusivity in a wide range in kinematics.

The first observation of the $\sin(\phi)$ -dependence for the $\bar{e}p \rightarrow e'p'\gamma$ process as signature of the interference of the DVCS and Bethe-Heitler amplitudes came from the CLAS (Stepanyan et al., 2001) and HERMES (Airapetian et al., 2001) detectors, while the H1 (Adloff et al., 2001) and ZEUS (Chekanov et al., 2003) collaborations measured, for the first time, the DVCS cross sections with both electron and positron beams on unpolarized protons in the kinematic domain of $x_B < 0.01$.

These initial results triggered the development of a worldwide dedicated experimental program to measure the DVCS process with high precision with HERMES at HERA, Hall A and CLAS at JLab, and COMPASS at

CERN. This experimental program required major construction projects, and new detector and accelerator upgrades employing state-of-the-art technologies.

HERMES provided a set of observables with different experimental conditions, electron and positron beams with both longitudinal and transverse spin polarizations for the lepton and proton (Airapetian et al., 2011). These data had important impact in the initial development and constraint of GPD models and the first global fits. Although HERMES was able to provide a complete set of DVCS measurements, the HERA machine operated at very low luminosity providing only low-statistics results until HERMES ended operation in 2007.

The COMPASS experiment took first DVCS data in a pilot run in 2012 with 160 GeV of oppositely polarised μ^+ and μ^- beams (Akhunzyanov et al., 2019). The average of the measured μ^+ and μ^- cross sections allows for the determination of $\text{Im}\mathcal{H}$. Results from an order of magnitude higher statistics obtained in 2016 and 2017 will soon be available. With these new data, the difference of μ^+ and μ^- cross sections can also be formed to provide access to $\text{Re}\mathcal{H}$.

In the 6 GeV era of JLab, dedicated DVCS experiments were designed and performed at low to moderate Q^2 in the region $x_B \approx 1/3$ involving modest upgrades to the detectors and the operating luminosity. The first dedicated experiment was the DVCS cross section measurements in Hall A, resulting in a first Q^2 -scaling test (Camacho et al., 2006).

Special detector configurations were incorporated with the construction of new equipment that doubled the luminosity the CLAS detector is able to operate at, to $2 \times 10^{34} \text{ cm}^{-2} \text{ s}^{-1}$. The CLAS collaboration has measured DVCS beam spin asymmetries and cross sections (Girod et al., 2008; Jo et al., 2015) and longitudinally polarized target-spin asymmetries (Chen et al., 2006; Pisano et al., 2015; Seder et al., 2015). The high statistical accuracy of the data collected in the large kinematic range of CLAS was essential for the first extraction of information on the proton D -term. This goes beyond the tomographic imaging with GPDs, and opened up the experimental investigation of the gravitational structure of the proton. The details of the high-level analysis will be described in the second part of this section.

One of the primary motivations of the 12 GeV energy upgrade at JLab was the study of the 3D structure of the nucleon by measurement of deeply exclusive processes with DVCS as the flagship program. In addition to the accelerator upgrade, this required a major upgrade to the experimental equipment from CLAS to CLAS12 (Burkert et al., 2020) with an order of magnitude increase in luminosity and an upgrade of Hall C. A comprehensive DVCS program has been approved as a major part of the 12 GeV science program. It incorporates experiments with polarized electron beams and energies from 6 to 11 GeV, longitudinally polarized hy-

drogen and deuterium targets, as well as conditionally approved measurements with transversely polarized proton targets, and with positron beams.

The first high-precision results of DVCS cross sections measured at 12 GeV in Hall A, focused on high values of the Bjorken variable x_B , have been published (Georges et al., 2022). The results of beam-spin asymmetry measurements at different energies with CLAS12 are in the public domain (Christiaens et al., 2022). The comprehensive DVCS measurements expected from JLab with the 12 GeV capabilities will significantly improve our understanding of the mechanical structure of the proton.

B. First extraction of the proton GFF $D_q(t)$

In this section, the data and procedure used in (Burkert et al., 2018) to obtain the first determination of the quark contribution to the D -term of the proton are described. This work is based on two main pieces of experimental information from the CLAS detector at JLab (Mecking et al., 2003), namely the beam-spin asymmetry (BSA) measured with spin-polarized electron beams, and the unpolarized cross section for DVCS on the proton.

The polarization asymmetries and differential cross sections have been used to extract the imaginary and real parts of the CFF \mathcal{H} respectively. Using the dispersion relation technique to determine the subtraction term $\mathcal{C}_{\mathcal{H}}(t)$ requires the full integral over $0 \leq \xi \leq 1$ at fixed t to be evaluated. As this process requires an extrapolation to both $\xi = 0$ and to $\xi = 1$ that are unreachable in experiments, a parameterization of the ξ -dependence of $\text{Im}\mathcal{H}$ close to these limits must be incorporated when fitting the data.

In the first step, local fits of the BSA (Girod et al., 2008) and of the unpolarized differential cross sections (Jo et al., 2015) for DVCS were performed to estimate $\text{Im}\mathcal{H}(\xi, t)$ and $\text{Re}\mathcal{H}(\xi, t)$ at fixed kinematics in ξ and t in the ranges covered by the data. The BSA is defined as

$$A_{LU}(\xi, t) = \frac{N^+(\xi, t) - N^-(\xi, t)}{N^+(\xi, t) + N^-(\xi, t)}, \quad (36)$$

where N^+ and N^- refer to the measured event rates at electron helicity +1 and -1, respectively.

The experimentally-measured BSA in $\bar{e}p \rightarrow ep\gamma$ contains not only the DVCS term, with the photon generated at the proton vertex, but also the Bethe-Heitler term with the photon generated at the incoming or scattered electron, respectively (see Fig. 2). Both have the same final state and thus interfere. They generate a $\sin \phi$ -dependent interference contribution as seen in Fig. 5. The DVCS term is dominated by the CFF $\text{Im}\mathcal{H}$ and the Bethe-Heitler term is real and is given by the elastic electromagnetic FFs.

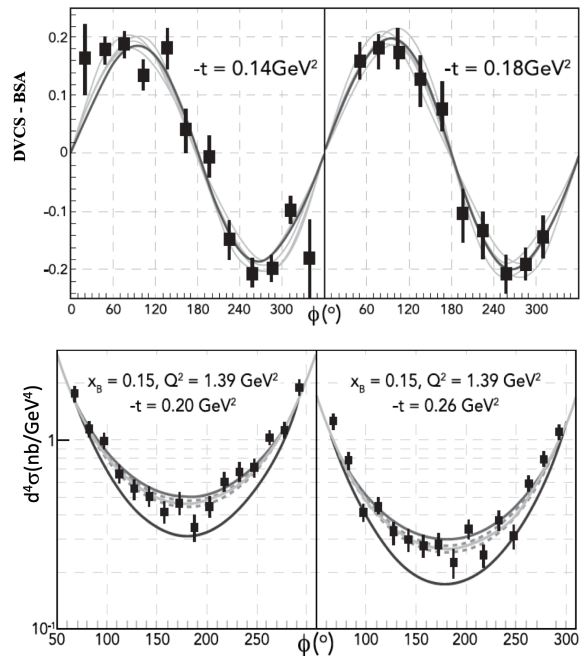


FIG. 5 Top: The expected $\sin \phi$ dependence is fit to the data. The thick solid lines are the global fits using the parameterization according to (37). The thin solid lines represent local fits. The thin gray lines represent estimates of the systematic uncertainties. Bottom: The unpolarized cross section at fixed ξ and Q^2 for different t values. The azimuthal ϕ angle dependence of the cross section is fitted to the experimental data. The thin solid line is the global fit. The thin gray lines represent local fits with dashed lines showing the systematic uncertainties. The thick black lines show the Bethe-Heitler contributions. Note the logarithmic vertical scale.

It is important to note that this analysis does not rely on extracted cross sections but on asymmetries of event rates in specific bins. This is an essential advantage as it avoids accounting for systematic uncertainties that must be included in the cross section extraction. The uncertainties in $A_{LU}(\xi, t)$ are dominated by statistics rather than systematic uncertainties, which determines the local values of $\text{Im}\mathcal{H}$ very precisely as can be seen in the top panel of Fig. 5, which shows the BSA and the differential cross sections for selected kinematic bins.

In the second step, the $\text{Im}\mathcal{H}(\xi, t)$ are fit with the functional form used in global fits (Kumericki et al., 2016; Müller et al., 2014) with the parameters fit to the local CLAS data. The imaginary part is written as:

$$\text{Im}\mathcal{H}(\xi, t) = \frac{\mathcal{N}}{1 + \xi} \frac{\left(\frac{2\xi}{1+\xi}\right)^{-\alpha(t)} \left(\frac{1-\xi}{1+\xi}\right)^b}{\left(1 - \frac{1-\xi}{1+\xi} \frac{t}{M^2}\right)^p}, \quad (37)$$

where \mathcal{N} is a free normalization constant, $\alpha(t)$ is fixed from small- x Regge phenomenology as $\alpha(t) = 0.43 + 0.85 t \text{ GeV}^{-2}$, b is a free parameter controlling the large- x behavior, p is fixed to 1 for the valence quarks, and M is a free parameter controlling the t -dependence.

The real and imaginary part are fit together including the subtraction term in the dispersion relation (32). Fig. 6 compares the local fit with the global fit for one of the t values. The global and local fits show good agreement in ξ and t kinematics where they overlap.

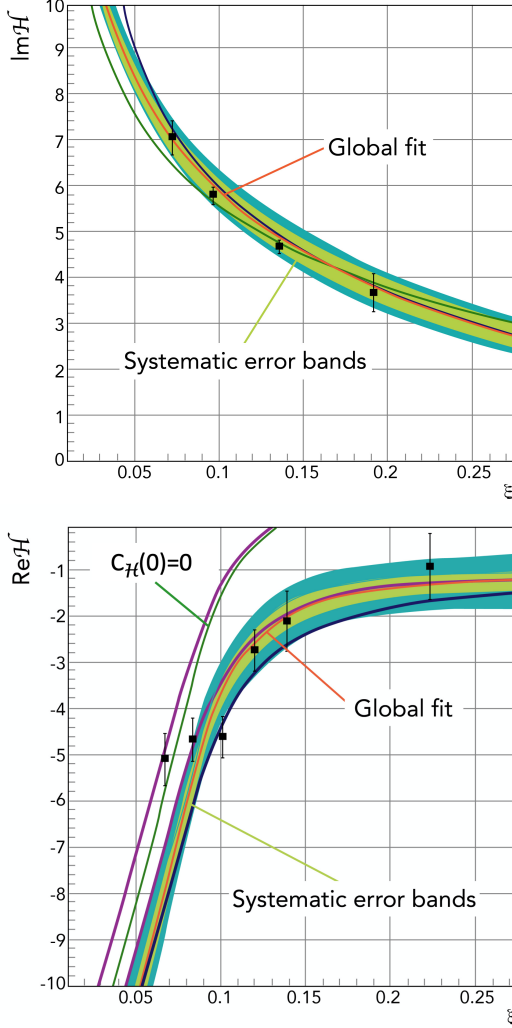


FIG. 6 Top: The $\text{Im}\mathcal{H}$ data points are plotted as function of ξ from local fits to the A_{LU} data (Girod et al., 2008) for $-t = 0.13\text{--}0.15$ GeV^2 . The red line is the global fit constrained by the local data points. The light-green error band is due to the uncertainty of the other CFFs. The outer dark-green band shows the total systematic uncertainty to the imaginary part of the fit. The upper and lower solid lines are due to uncertainties from possibly steeper or less steep ξ -dependences of $\text{Im}\mathcal{H}$. Bottom: $\text{Re}\mathcal{H}$ data as extracted from unpolarized cross section data (Jo et al., 2015). The central red curve shows the result of the global fit with the dispersion relation applied and the fit parameters of the multipolar form for $\mathcal{C}_{\mathcal{H}}(t)$. The other colored lines/bands describe the same contribution as for $\text{Im}\mathcal{H}$ propagated with the dispersion relation. The black curve separated from the error bands shows the real part of the amplitude computed from the imaginary part using the dispersion relation and setting $\mathcal{C}_{\mathcal{H}}(0)$ to zero. The difference of solid red and solid black line shows the effect of the subtraction term. Note that all markers in $\text{Re}\mathcal{H}$ contribute to the precision of a single $-t$ value in $\mathcal{C}_{\mathcal{H}}(t)$, resulting in a small fit uncertainty.

In the fit, $\mathcal{C}_{\mathcal{H}}(t)$ is obtained at fixed t . The results for

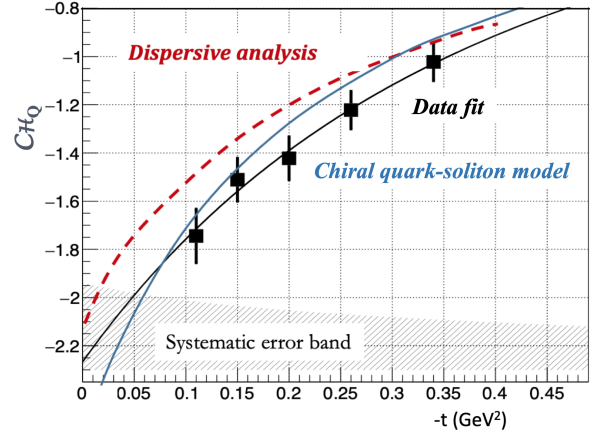


FIG. 7 The subtraction term $\mathcal{C}_{\mathcal{H}}(t)$ as determined from the dispersion relation in the global fit (markers). The uncertainties represent results of the fit errors. The hatched area at the bottom represents the estimated systematic uncertainties as described in Fig. 6 for one of the bins in $-t$. The dashed and solid-blue curves show the dispersive calculation (Pasquini et al., 2014) and chiral quark-soliton model predictions (Goeke et al., 2007a), respectively.

the subtraction term and the fit to the multipole form

$$\mathcal{C}_{\mathcal{H}}(t) = \mathcal{C}_{\mathcal{H}}(0) \left[1 + \frac{(-t)}{M^2} \right]^{-\lambda} \quad (38)$$

are displayed in Fig. 7, where $\mathcal{C}_{\mathcal{H}}(0)$, λ and M^2 are the fit parameters, with their values found to be:

$$\begin{aligned} \mathcal{C}_{\mathcal{H}}(0) &= -2.27 \pm 0.16 \pm 0.36, \\ M^2 &= 1.02 \pm 0.13 \pm 0.21 \text{ GeV}^2, \\ \lambda &= 2.76 \pm 0.23 \pm 0.48. \end{aligned} \quad (39)$$

The first error is the fit uncertainty, and the second error is due to the systematic uncertainties. Adding the fit errors for $\mathcal{C}_{\mathcal{H}}(0)$ and the systematic errors in quadrature $\sigma_{\mathcal{C}_{\mathcal{H}}(0)} = \sqrt{0.16^2 + 0.36^2} \approx 0.39$, the significance S of the knowledge of the subtraction term is:

$$S = \frac{\mathcal{C}_{\mathcal{H}}(0)}{\sigma_{\mathcal{C}_{\mathcal{H}}(0)}} \approx 5.8. \quad (40)$$

More flexible analyses based on unconstrained artificial neural network techniques (Dutrieux et al., 2021; Kumerički, 2019) find however that a more conservative extraction of the subtraction constant from the currently available experimental data remains compatible with zero within large uncertainties.

In the analysis of (Burkert et al., 2018), the term $d_3^q(t)$ and other higher-order terms have been omitted in the expansion (34) to extract the GFF $D_q(t)$. The estimated effect is included in the systematic error analysis. It is also assumed that u and d quarks have the same first moments $d_1^u \approx d_1^d \approx d_1^{u+d}/2$, an assumption justified in the large- N_c limit (Goeke et al., 2001). Under these

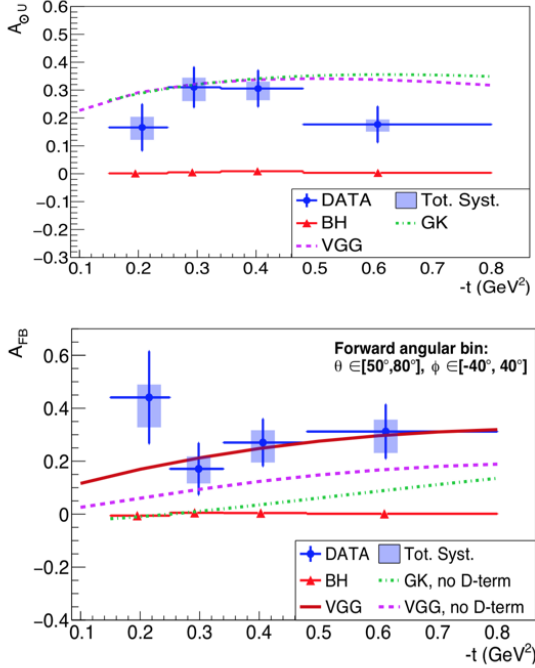


FIG. 8 The TCS polarized BSA (top) and the TCS A_{FB} (bottom) for an average 1.8 GeV mass of the time-like photon $M_{e^+e^-}$. A value for A_{LU} of (20-25)% is consistent with what is measured in DVCS and projects out $\text{Im}\mathcal{H}$. The FBA projects out $\text{Re}\mathcal{H}$ that relates directly to the protons $D_q(t)$ -term. The data require the presence of the D -term as seen in the difference of the dashed magenta line and the solid red line. At the kinematics of the data in Fig. 7, about half of the asymmetry may be due to the D -term when comparing calculations without and with the D -term (Pasquini *et al.*, 2014; Vanderhaeghen *et al.*, 1999).

approximations, it follows from (35) that

$$\mathcal{C}_{\mathcal{H}}(t) \approx \frac{10}{9} d_1^{u+d}(t) = \frac{25}{18} D_{u+d}(t). \quad (41)$$

The truncation in (34) leads to a systematic uncertainty of a priori unknown magnitude. For $Q^2 \rightarrow \infty$, the higher order terms d_3^q, d_5^q, \dots vanish. But at the Q^2 that can be reached in the current experiments, they are not necessarily negligible. The results of the chiral quark-soliton model, which predicts values of d_1^{u+d} close to findings in the experimental analysis (Goeke *et al.*, 2007a), can be used to estimate the contribution of the d_3^q term. At the kinematics relevant for this analysis a ratio $d_3^{u+d}/d_1^{u+d} \approx 0.3$ was found (Kivel *et al.*, 2001). A systematic uncertainty of $\delta(d_1^{u+d})/d_1^{u+d} = \pm 0.30$ has therefore been included into the results of (Burkert *et al.*, 2018) for $d_1^{u+d}(t)$.

One may ask if the first two terms in the Gegenbauer polynomial expansion $d_1^q(t)$ and $d_3^q(t)$ could be separated in some way to reduce the systematics. This has been studied in (Dutrieux *et al.*, 2021) by including the Q^2 -

evolution into the phenomenological analysis. It was found that, assuming the same t -dependence, the two terms cannot currently be separated given the limited range in Q^2 covered by the data. In the future one may expect Lattice QCD to be able to provide a model-independent evaluation of this higher-order contribution.

To conclude this section, the determination of $\mathcal{C}_{\mathcal{H}}(t)$ suggests that the quark contribution $\sum_q D_q(t)$ to the proton's GFF $D(t)$ is non-zero and large. These results have been supported in a recent paper on the first measurement of TCS (Chatagnon *et al.*, 2021) as shown in Fig. 8, where the contribution of the D -term to the forward-backward asymmetry is seen to be significant. Moreover, predictions in the chiral quark-soliton model (Goeke *et al.*, 2007a) and from dispersive analysis (Pasquini *et al.*, 2014) shown in Fig. 7 are consistent with the results discussed here within the systematic uncertainties.

C. Future experimental developments to access GFFs.

As discussed in section III, measurements of DVCS have so far been most effective in obtaining information related to GPDs. However, there are different experimental processes that may be employed to provide additional, or independent, information on the GPDs and GFFs.

Implementation of a high-duty-cycle positron source, both polarized and unpolarized (Abbott *et al.*, 2016), at JLab would significantly enhance its capabilities in the extraction of the CFF $\text{Re}\mathcal{H}(\xi, t)$ and thus of the gravitational form factor $D_q(t)$ and of the mechanical properties of the proton.

The time-like Compton scattering process will be measured in parallel to the DVCS process employing the large acceptance detector systems such as CLAS12 (Burkert *et al.*, 2020). The TCS event rate is much reduced compared to DVCS and requires higher luminosity for similar sensitivity to \mathcal{H} . In experiments employing large acceptance detector systems, both DVCS and TCS processes are measured simultaneously, in quasi-real photo-production at very small $Q^2 \rightarrow 0$, and in real photo-production, where the external production target acts as a radiator of real photons that undergo TCS further downstream in the same target cell. The science program in Hall D at JLab has measured the energy-dependence of J/Ψ production with real photon beams (Ali *et al.*, 2019), where data close to threshold have been employed for the extraction of the gluon scalar radius (Kharzeev, 2021) of the proton.

The DDVCS process enables access to GPDs in their full kinematic dependencies on x, ξ, t , see Sec. III. At the same time it is reduced in rate by orders of magnitude compared to DVCS (Kopeliovich *et al.*, 2010) requiring higher luminosity than is currently achievable. Nevertheless, special equipment that would comply with such

requirements has been proposed (Chen et al., 2014). Such measurements are currently planned at JLab in Hall A and Hall B.

Finally, an energy-doubling of the existing electron accelerator at JLab is currently under consideration (Arrington et al., 2022). This upgrade would extend the DVCS program to higher Q^2 and lower x_B and better link the DVCS measurements at the current 12 GeV operation to the kinematic reach that will be available at the Electron-Ion Collider, a flagship future facility in preparation at the Brookhaven National Laboratory (discussed further below). It will also more fully open the charm sector to access the gluon GFFs. The energy upgrade will be essential for a comprehensive measurement of deeply exclusive meson production, both in the vector meson and the pseudo-scalar meson sector.

D. Other phenomenological studies

The first extraction of the π^0 GFFs in the time-like region (Kumano et al., 2018) based on the process $\gamma\gamma^* \rightarrow \pi^0\pi^0$, depicted in Fig. 3, which was measured in the Belle experiment in e^+e^- collisions (Masuda et al., 2016). For the quark contribution to the π^0 D -term the value $\sum_q D_q(0) \approx -0.75$ was reported, but systematic uncertainties have not been estimated. It has recently been observed in (Lorcé et al., 2022a) that kinematical corrections may significantly impact the extraction of generalized distribution amplitudes from experimental data and should be taken into account in future analyses.

Phenomenological studies of gluon GFFs have been presented in (Kou et al., 2021; Wang et al., 2022) where the gluon $D_G(t)$ form factor of the proton was extracted from J/Ψ threshold photoproduction data. (For remarks on the theoretical status of this process see Sec. III.C.) A similar study for the lighter ϕ -meson was presented in (Hatta and Strikman, 2021).

V. THEORETICAL RESULTS

GFFs were introduced by (Kobzarev and Okun, 1962) who considered spin-0 and spin- $\frac{1}{2}$ particles and parity-violating weak effects (not discussed here), proved the vanishing of proton's anomalous gravitomagnetic moment $B(0) = 0$, and showed that one would need energies around the Planck scale to measure GFFs in gravitational interactions. This section presents an overview of GFFs from the theory perspective with particular focus on $D(t)$, the least known of the total GFFs.

A. Chiral symmetry and the D -term of the pion

GFFs received little attention from the community until it was realized that matrix elements such as

$\langle \pi, \pi | T^{\mu\nu} | 0 \rangle$ enter the QCD description of hadronic decays of charmonia (Novikov and Shifman, 1981; Voloshin and Zakharov, 1980) or the decay of a hypothetical light Higgs boson, an idea entertained in the early 1990s when the possibility of a light Higgs was not yet experimentally excluded (Donoghue et al., 1990). These matrix elements are related to pion GFFs in the timelike region $t > 0$.

In general, hadronic EMT matrix elements cannot be computed analytically, but the pion is a notable exception. The QCD Lagrangian (1) exhibits a classical symmetry under global left- and right-handed rotations in the flavor space of up, down and strange quarks. This symmetry is approximate due to the small but non-zero quark masses m_q . If this symmetry were realized in nature, then for instance the nucleon $N(940)$ and its negative-parity partner, the $N(1535)$, should have the same masses modulo small corrections due to the small m_q . However, the $N(1535)$ is almost 600 MeV heavier than the nucleon, an effect that cannot be attributed to current quark mass effects. The phenomenon that a symmetry of the Lagrangian is not realized in the particle spectrum is known as spontaneous symmetry breaking (Nambu and Jona-Lasinio, 1961a,b). It is accompanied by the emergence of massless Goldstone bosons, corresponding in QCD to pions, kaons, and η -mesons, which are not massless but are very light compared to other hadrons.

In theoretical calculations, chiral symmetry is a powerful tool allowing one to evaluate the matrix elements of Goldstone bosons in the chiral limit (and for $t \rightarrow 0$). In this way, one obtains for the pion (and kaon and η) D -term

$$\lim_{m_\pi \rightarrow 0} D_\pi = -1. \quad (42)$$

Deviations from the chiral limit are systematically calculable in chiral perturbation theory (Donoghue and Leutwyler, 1991) and are expected to be small for pions and more sizable for kaons and the η (Hudson and Schweitzer, 2017). The gravitational interactions of Goldstone bosons were studied by (Leutwyler and Shifman, 1989; Voloshin and Dolgov, 1982).

B. GFFs in model studies

Interest in GFFs was once again renewed after it was shown that they can be inferred from hard-exclusive reactions via GPDs and play a key role for the understanding of the mass and spin structure of the proton, see Sec. II, and further stimulated by their interpretation in terms of forces inside hadrons (Polyakov, 2003). The first model study of proton GFFs was presented by (Ji et al., 1997) in the bag model, followed by works in the chiral quark-soliton model (Goeke et al., 2007a,b; Kim and Kim, 2021; Ossmann et al., 2005; Petrov et al., 1998; Schweitzer et al., 2002; Wakamatsu, 2007) and Skyrme

models (Cebulla et al., 2007; Jung et al., 2014a; Perevalova et al., 2016).

Extensive GFF model studies for the nucleon and other hadrons were presented in light-front constituent quark models (Pasquini and Boffi, 2007; Sun and Dong, 2020), diquark approaches (Chakrabarti et al., 2020; Choudhary et al., 2022; Fu et al., 2022; Hwang and Mueller, 2008; Kumar et al., 2017), holographic AdS/QCD models (Abidin and Carlson, 2008, 2009; Brodsky and de Tera-mond, 2008; Chakrabarti et al., 2015; Fujita et al., 2022; Mamo and Zahed, 2020, 2021, 2022; Mondal, 2016; Mondal et al., 2016), a large- N_c bag model (Lorcé et al., 2022b; Neubelt et al., 2020), a cloudy bag model (Owa et al., 2022), light-cone QCD sum rules (Aliev et al., 2021; Anikin, 2019; Azizi and Özdem, 2020, 2021; Özdem and Azizi, 2020), the Nambu–Jona-Lasinio model (Freese et al., 2019), chiral quark-soliton model with strange and heavier quarks (Ghim et al., 2022; Kim et al., 2021; Won et al., 2022), a dual model with complex Regge trajectories (Fiore et al., 2021), and in an instant-form relativistic impulse approximation approach (Krutov and Troitsky, 2021, 2022). Algebraic GPD Ansätze were used to shed light on pion and kaon GFFs (Raya et al., 2022) and toy models (Kim et al., 2022a) as well as light-cone convolution models (Freese and Cosyn, 2022a) were used to study the deuteron GFFs.

The D -terms of nuclei were studied in the liquid-drop model (Polyakov, 2003), revealing that for nuclei $D(0) \propto A^{7/3}$ grows strongly with mass number A . Studies in the Walecka model (Guzey and Siddikov, 2006) support this prediction which can be tested in DVCS experiments with nuclear targets. Different results were obtained in a non-relativistic nuclear spectral function approach (Liuti and Taneja, 2005). Nuclear medium effects were investigated in Skyrme model frameworks (Jung et al., 2014b; Kim et al., 2012, 2022b).

The GFFs of a constituent quark were studied in a light-front Hamiltonian approach (More et al., 2022) which, after rescaling and regularization of infrared divergences, reproduces QED results for an electron (Metz et al., 2021). GFFs of the photon in QED were studied in (Freese and Cosyn, 2022b; Friot et al., 2007; Gabdrakhmanov and Teryaev, 2012; Polyakov and Sun, 2019). An insightful model for composite particles is the Q -ball system where stable, metastable, unstable states were investigated, showing that, among all studied particle properties, $D(0)$ is most sensitive to details of the dynamics (Cantara et al., 2016; Mai and Schweitzer, 2012a,b). Remarkably, the same conclusions were obtained in the bag model where, e.g., for the N^{th} highly excited nucleon state the mass increases as $M \propto N^3$ whereas $D(0) \propto N^8$ grows much more strongly with N (Neubelt et al., 2020).

C. Limits in QCD and dispersion relations

Model-independent results for GFFs can be obtained in certain limiting situations in QCD, e.g., when the number of colors $N_c \rightarrow \infty$ or when $|t|$ becomes very small or very large, and through the use of dispersion relation methods. These methods are complementary to the non-perturbative lattice QCD methods which are reviewed in the next section.

In the large- N_c limit of QCD, baryons are described as solitons of mesonic fields (Witten, 1979). Large- N_c QCD has not been solved (in 3+1 dimensions) and the soliton field is not known (though it can be modelled). Nontrivial results can, however, be derived based on the known symmetries of the large- N_c soliton field which are generally well-supported in nature (Dashen et al., 1994) despite $N_c = 3$. The relations of the GFFs of the nucleon and Δ were studied in the large- N_c limit of QCD in (Panteleeva and Polyakov, 2020). The GFFs of the Δ are difficult to measure, but such relations can be tested, e.g., in soliton models like the chiral quark-soliton model or Skyrme model (mentioned in the previous subsection) or in lattice QCD, discussed in the next section.

At small $|t|$, one can use chiral perturbation theory, where one writes down an effective Lagrangian in terms of hadronic degrees of freedom with the most general interactions allowed by chiral symmetry, and free parameters which can be inferred from comparison of observable quantities with experiment. A pioneering study to lowest order in chiral perturbation theory was presented in (Belitsky and Ji, 2002) and studies at next-to-leading order (Diehl et al., 2006) have been completed in (Alharazin et al., 2020). In this way, one can obtain valuable model-independent information on the t -dependence of GFFs for small t . For instance, for the nucleon the slope of $D(t)$ at $t = 0$ diverges in the chiral limit as

$$\left. \frac{d}{dt} D(t) \right|_{t=0} = -\frac{g_A^2 M_N}{40\pi f_\pi^2 m_\pi} + \dots, \quad (43)$$

where $g_A = 1.26$ is the isovector axial constant, $f_\pi = 93$ MeV is the pion decay constant, m_π is the pion mass, and the dots indicate (finite) higher-order chiral corrections. Such results are reproduced in chiral soliton models (Cebulla et al., 2007; Goeke et al., 2007a). The value of the D -term cannot be determined exactly in chiral perturbation theory for hadrons other than Goldstone bosons. It is, however, possible to derive an upper bound, e.g., for the nucleon $D/M_N \leq -(1.1 \pm 0.1) \text{ GeV}^{-1}$ in the chiral limit (Gegelia and Polyakov, 2021). The GFFs of the ρ -meson (Epelbaum et al., 2022) and Δ -resonance (Alharazin et al., 2022) have also been studied in chiral perturbation theory.

Model-independent results for GFFs can also be derived for asymptotically large momentum transfers using power counting and perturbative QCD methods (Tanaka, 2018; Tong et al., 2021, 2022). For instance, the proton

GFFs $A_a(t)$ for quarks and gluons behave like $1/t^2$ at large $(-t) \rightarrow \infty$. Since QCD factorization of hard exclusive processes requires $(-t) \ll Q^2$ and Q^2 is in practice often not large in current experimental settings, such results provide important theoretical guidelines to extrapolate to larger $|t|$. However, based on experience with analogous perturbative QCD predictions for the electromagnetic pion form factor, see e.g. (Horn and Roberts, 2016) for a review, it is difficult to anticipate how large the momentum transfer t must be for a form factor to reach the asymptotic regime.

A theoretical study of the quark contribution to the nucleon GFF $D_q(t)$ in the range $0 < (-t) < 1 \text{ GeV}^2$ was presented in (Pasquini *et al.*, 2014) based on dispersion theory methods which rely on general principles like relativity, causality and unitarity. This approach does not require modelling other than making use of available information on pion-nucleon partial-wave helicity amplitudes and relying on mild assumptions like the saturation of the t -channel unitarity relation in terms of the two-pion intermediate states or input pion PDF parametrizations.

D. Lattice QCD

Complementing the insights gained from models of proton and nuclear structure, numerical lattice QCD calculations give direct and controllable QCD predictions for matrix elements of the EMT operator. In particular, lattice QCD is the only known systematically improvable approach to computing observables in QCD in the low-energy (non-perturbative) regime. The approach proceeds via a discretisation of the QCD Lagrangian (1) onto a Euclidean space-time lattice, with a finite lattice spacing which is not physical but acts as a method of regularisation of the theory. Calculations then proceed via Monte-Carlo integration of the high-dimensional discretised path-integral; continuum QCD results are recovered in the limit of vanishing lattice discretisation scale, infinite lattice volume, and precise matching of the bare quark masses to reproduce simple physical observables. By this approach, matrix elements of local operators, such as the separated quark and gluon components of the EMT in proton or nuclear states, may be computed directly.

In the current era of precision lattice QCD calculations of proton structure, particular efforts have been made to determine the complete decomposition of the proton’s spin and momentum into individual quark and gluon contributions with high precision and systematic control. For example, recent lattice QCD studies have isolated all angular momentum components in the kinetic (or Ji) decomposition (Alexandrou *et al.*, 2020a; Wang *et al.*, 2021), with $\approx 10\%$ uncertainty in the total quark and gluon contributions; the results from one collaboration are shown in Fig. 9. This example illustrates the

complementarity between theory and experiment in this area; flavour separation in lattice QCD calculations is in principle more straightforward, although some contributions, such as those from gluons or arising from “disconnected” contributions, e.g. strange and charm quarks in the proton, are difficult to compute because of signal-to-noise challenges. Computing the gluon spin and orbital angular momentum in the Jaffe-Manohar decomposition introduces additional challenges to the lattice QCD approach, but first results have been achieved based on constructions using both local and non-local operators (Engelhardt *et al.*, 2020; Yang *et al.*, 2017).

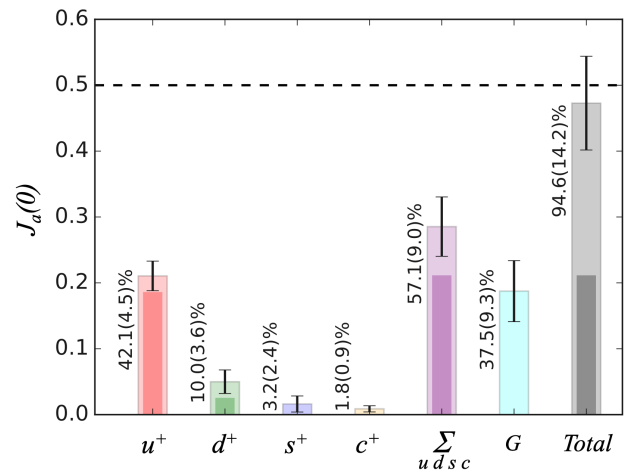


FIG. 9 Proton spin decomposition computed in lattice QCD in (Alexandrou *et al.*, 2020a), given in the $\overline{\text{MS}}$ scheme at 2 GeV. Each component includes the contribution of both the quarks and antiquarks ($q^+ = q + \bar{q}$); outer (inner) coloured bars denote the total (purely connected) contributions.

In the same vein, precise decompositions of the quark and gluon contributions to the proton’s momentum, which are related to the mass decomposition, have been achieved with complete systematic control in the same computational frameworks that yielded the spin decomposition (Alexandrou *et al.*, 2020a; Wang *et al.*, 2021). Contributions from the trace anomaly to the proton’s mass decomposition are more difficult to compute directly with systematic control, but have also been constrained using the mass sum rule (20); Fig. 10 shows the first insight from lattice QCD into the pion mass (or quark mass) dependence of the proton’s mass decomposition given in (24) (Yang *et al.*, 2018b). It is particularly notable that while the quark scalar condensate contribution varies rapidly with quark mass, the other contributions, including that of the trace anomaly, remain approximately constant.

While local matrix elements in nuclear states can in principle be computed in lattice QCD in the same way as in the proton state, such calculations face significant practical and computational challenges, in particular compounding factorial and exponential growth in

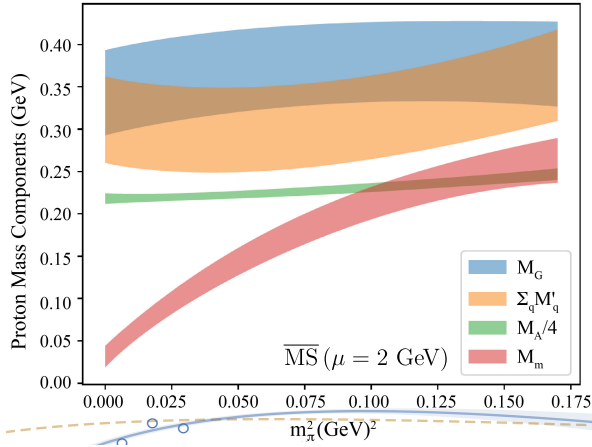


FIG. 10 Ji's mass decomposition (24) for a proton computed in lattice QCD in (Yang et al., 2018b) at a scale $\mu = 2$ GeV, as a function of the pion mass.

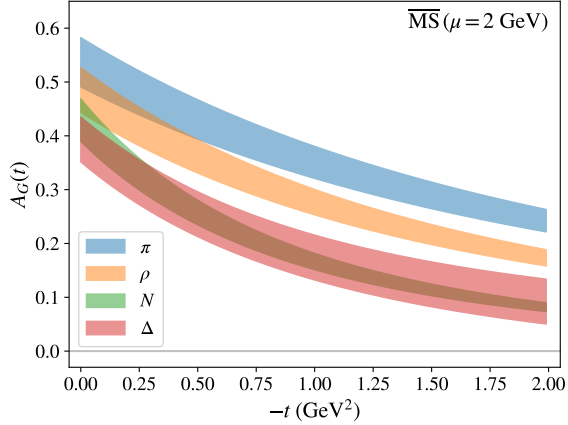


FIG. 11 $A_G(t)$ GFF for various hadrons from (Pefkou et al., 2021), with quark masses corresponding to a larger-than-physical value of the pion mass of 450MeV.

computational cost with the atomic number of the nuclear state. To date, a single first-principles calculation of isovector quark momentum fraction $A_{u-d}(0)$ in ^3He (Detmold et al., 2021b) has been achieved; despite significant systematic uncertainties, including the result into global fits of experimental lepton-nucleus scattering data yields improved constraints on the nuclear parton distributions. Over the coming decade, it can be anticipated that the control and precision achieved in first-principles calculations of simple aspects of the gravitational structure of the proton will be extended to nuclear states. Beyond forward-limit matrix elements, lattice QCD has also been used to compute the quark and gluon GFFs of the proton and other hadrons. Such calculations are computationally more demanding than those needed to constrain the forward-limit components, and statistical uncertainties increase with $|t|$. As a result, these studies have not yet achieved the same level of systematic

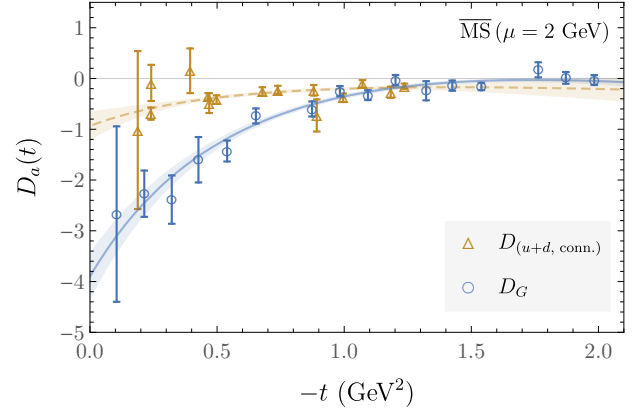


FIG. 12 $D_G(t)$ and $D_{u+d}(t)$ GFF for the proton from (Shanahan and Detmold, 2019a), with quark masses corresponding to a pion mass of 450MeV.

control as the spin and mass decomposition. Nevertheless, the quark contributions to the proton's GFFs (and those of other hadrons such as the pion) have been computed with $|t| \lesssim 1$ GeV² (Alexandrou et al., 2020a, 2017, 2020c, 2018; Bali et al., 2016; Brommel et al., 2006; Brommel, 2007; Hagler et al., 2008; Yang et al., 2018a,b). The gluon contributions to the proton's GFFs are far less well-constrained, and almost all calculations to date have been performed with quark masses corresponding to larger-than-physical values of the pion mass (Detmold et al., 2017; Pefkou et al., 2021; Shanahan and Detmold, 2019a,b). Nevertheless, the gluon GFFs with $|t| \lesssim 2$ GeV² were computed for a range of hadrons in (Pefkou et al., 2021), allowing qualitative comparisons of their t -dependence as illustrated in Fig. 11. Of particular recent interest has been the $D(t)$ GFF, which does not have a sum-rule constraint in the forward limit; a comparison between lattice QCD calculations of the quark and gluon contributions is illustrated in Fig. ?? **PSch:** [?]

In contrast to local matrix elements, matrix elements defined with light-cone separations, yielding e.g. the x -dependence of GPDs, can not be directly computed in Euclidean spacetime, but must be approached by indirect means. Significant developments over the last two decades have yielded a range of complementary approaches to direct calculations of GPDs themselves in the lattice QCD framework (Chambers et al., 2017; Constantinou et al., 2021; Detmold et al., 2021a; Detmold and Lin, 2006; Ji, 2013; Ma and Qiu, 2018; Radyushkin, 2017). Given the significant technical and computational challenges of these approaches, the first lattice QCD studies of the x -dependence of the proton GPDs were achieved only recently in 2020 (Alexandrou et al., 2020d; Lin, 2021). Calculations with complete systematic control will require continued efforts over the coming years. Even more recently, the first QCD calculation of the chiral-odd transversity GPDs of the proton (Alexan-

drou *et al.*, 2022) has been achieved. While systematic uncertainties remain to be controlled in this case also, these early results already showcase the complementarity between theory and experiment which will continue to grow in the coming years; while they are no more difficult to compute in the lattice QCD approach than the helicity-preserving distributions, the transversity GPDs cannot be measured in DVCS (but can in deeply virtual meson production), and are less constrained experimentally than their chiral-even counterparts.

VI. INTERPRETATION

A lot of interest in GFFs comes from the fact that they contain information on the spatial distributions of energy, angular momentum, and internal forces via an appealing interpretation which is reviewed here.

A. The static EMT

The 3D interpretation of the information encoded by GFFs provides analogies to intuitive concepts such as pressure. The interpretation is carried out in the Breit frame, where $\Delta^\mu = (0, \vec{\Delta})$ and $P^\mu = (E, \vec{0})$ with $E = (M_N^2 + \frac{1}{4}\vec{\Delta}^2)^{1/2}$, by introducing the static EMT

$$\mathcal{T}^{\mu\nu}(\vec{r}) = \int \frac{d^3\Delta}{(2\pi)^3 2E} e^{-i\vec{\Delta}\cdot\vec{r}} \langle p' | T^{\mu\nu}(0) | p \rangle, \quad (44)$$

where for brevity the dependence of $\mathcal{T}^{\mu\nu}(\vec{r})$ on the nucleon polarization (Polyakov, 2003) is suppressed. A 2D interpretation can also be carried out in other frames (Freese and Miller, 2021, 2022; Lorcé *et al.*, 2019) with Abel transformations allowing one to relate 2D and 3D interpretations (Panteleeva and Polyakov, 2021).

Considering 2D EMT distributions for a nucleon state boosted to the infinite-momentum frame has the advantage that in this case the transverse center of momentum of the nucleon is well defined (Burkardt, 2000). In other frames or in 3D, an exact probabilistic parton density interpretation does not hold in general. The reservations are analogous to those in the case of, e.g., the interpretation of the electric FF in terms of a 3D electrostatic charge distribution (and the definition of electric mean square charge radius which, despite all caveats, remains a popular concept, giving an idea of the proton's size). The 3D EMT description is nevertheless mathematically rigorous (Polyakov and Schweitzer, 2018b) and can be interpreted in terms of quasi-probabilistic distributions from a phase-space point of view (Lorcé, 2020; Lorcé *et al.*, 2019). A strict probabilistic interpretation is however justified for heavy nuclei and for the nucleon in the large- N_c limit, where recoil effects can be safely neglected (Goeke *et al.*, 2007a; Lorcé *et al.*, 2022b; Polyakov, 2003; Polyakov and Schweitzer, 2018b).

In (44) the total static EMT is considered, but one can also define separate quark and gluon static EMTs (Lorcé *et al.*, 2019; Polyakov, 2003). The meaning of the different components of the static EMT is intuitively clear, with $\mathcal{T}^{00}(\vec{r})$ denoting the energy distribution and $\mathcal{T}^{0k}(\vec{r})$ representing the spatial distribution of momentum. In the following sections the focus is on $\mathcal{T}^{ij}(\vec{r})$ which are perhaps the most interesting components of the static EMT, thanks to their relation to the stress tensor and the D -term.

B. The stress tensor and the D -term

The key to the mechanical properties of the proton is the symmetric stress tensor $\mathcal{T}^{ij}(\vec{r})$ given by (Polyakov, 2003)

$$\mathcal{T}^{ij}(\vec{r}) = \left(\frac{r^i r^j}{r^2} - \frac{1}{3} \delta^{ij} \right) s(r) + \delta^{ij} p(r) \quad (45)$$

with $s(r)$ known as the shear force (or anisotropic stress) and $p(r)$ as the pressure with $r = |\vec{r}|$. Both are connected by the differential equation $\frac{2}{3} \frac{d}{dr} s(r) + \frac{2}{r} s(r) + \frac{d}{dr} p(r) = 0$ and $p(r)$ obeys $\int_0^\infty dr r^2 p(r) = 0$ (von Laue, 1911), a necessary but not sufficient condition for stability. These relations originate from the EMT conservation expressed by $\nabla^i \mathcal{T}^{ij}(\vec{r}) = 0$ for the static EMT. The total D -term $D(0)$ can be expressed in terms of $p(r)$ and $s(r)$ in two equivalent ways,

$$D(0) = -\frac{4}{15} M_N \int d^3r r^2 s(r) = M_N \int d^3r r^2 p(r). \quad (46)$$

The form of the stress tensor (45) is valid for spin-0 and spin- $\frac{1}{2}$ hadrons; for higher spins see (Cosyn *et al.*, 2019; Cotogno *et al.*, 2020; Ji and Liu, 2021; Kim and Sun, 2021; Polyakov and Sun, 2019).

If the GFF $D(t)$ is known, then $s(r)$ and $p(r)$ are obtained as follows (Polyakov and Schweitzer, 2018b)

$$s(r) = -\frac{1}{4M_N} r \frac{d}{dr} \frac{1}{r} \frac{d}{dr} \tilde{D}(r), \quad (47)$$

$$p(r) = \frac{1}{6M_N} \frac{1}{r^2} \frac{d}{dr} r^2 \frac{d}{dr} \tilde{D}(r), \quad (48)$$

where $\tilde{D}(r) = \int \frac{d^3\Delta}{(2\pi)^3} e^{-i\vec{\Delta}\cdot\vec{r}} D(-\vec{\Delta}^2)$. If the separate $D_q(t)$ and $D_G(t)$ GFFs are known, “partial” quark and gluon shear forces $s_q(r)$ and $s_G(r)$ can be defined in analogy to (47). In order to define “partial” quark and gluon pressures, in addition to $D_q(t)$ and $D_G(t)$ knowledge of $\tilde{C}_q(t)$ and $\tilde{C}_G(t)$ is required. The latter are responsible for “reshuffling” of forces between the gluon and quark subsystems inside the proton (Polyakov and Son, 2018) and are difficult to access experimentally. The instanton vacuum model predicts $\tilde{C}_q(t)$ to be very small (Polyakov and Son, 2018) but other estimates indicate that it may be significant (Hatta *et al.*, 2018; Tanaka, 2022).

C. Normal forces and the sign of the D -term

The stress tensor $\mathcal{T}^{ij}(\vec{r})$ can be diagonalized, with one eigenvalue given by the normal force per unit area $p_n(r) = \frac{2}{3}s(r) + p(r)$ with the pertinent eigenvector \vec{e}_r . The other two eigenvalues are degenerate (for spin-0 and spin- $\frac{1}{2}$) and are known as tangential forces per unit area, $p_t(r) = -\frac{1}{3}s(r) + p(r)$, with eigenvectors which can be chosen to be unit vectors in the ϑ - and φ -directions in spherical coordinates (Polyakov and Schweitzer, 2018b).

The normal force appears when considering the force $F^i = \mathcal{T}^{ij}dS^j = p_n(r)dS e_r^i = [\frac{2}{3}s(r) + p(r)]dS e_r^i$ acting on a radial area element $dS^j = dS e_r^j$, where $e_r^j = r^j/r$. General mechanical stability arguments require this force to be directed towards the outside, or else the system would implode. This implies that the normal force per unit area must be positive

$$p_n(r) = \frac{2}{3}s(r) + p(r) > 0. \quad (49)$$

As an immediate consequence of (49) one concludes by means of Eq. (46) that (Perevalova et al., 2016)

$$D(0) < 0. \quad (50)$$

For hadronic systems like protons, hyperons, mesons or nuclei for which the D -term has been computed (in models, chiral perturbation theory, lattice QCD or by dispersive techniques, see Sec. V) or inferred from experiment (in the case of the proton and π^0 , see Sec. IV) it has always been found to be negative in agreement with (50).

The above definitions and conclusions are more than just a fruitful analogy to mechanical systems. At this point it is instructive to recall how one calculates the radii of neutron stars, which are amenable to an unambiguous 3D interpretation. In these macroscopic hadronic systems, general relativity effects cannot be neglected and are incorporated in the Tolman-Oppenheimer-Volkoff equation, which is solved by adopting a model for the nuclear matter equation of state. The solution yields (in our notation) $p_n(r)$ inside the neutron star as function of the distance r from the center. The obtained solution is positive in the center and decreases monotonically until it drops to zero at some $r = R_*$, and would be negative for $r > R_*$ corresponding to a mechanical instability. This is avoided and a stable solution is obtained by defining $r = R_*$ to be the radius of the neutron star, see for instance (Prakash et al., 2001). Thus, the point where the normal force per unit area drops to zero coincides with the “edge” of the system.

The proton has of course no sharp “edge”, being surrounded by a “pion cloud” due to which the normal force does not drop literally to zero but exhibits a Yukawa-type suppression at large r proportional to $\frac{1}{r^8} e^{-2m_\pi r}$ (Goeke et al., 2007a). In the less realistic but very instructive bag model, there is an “edge” at the bag boundary, where

$p_n(r)$ drops to zero (Neubelt et al., 2020). In contrast to the neutron star one does not determine the “edge” of the bag model in this way. Rather the normal force drops “automatically” to zero at the bag radius which reflects the fact that from the very beginning the bag model was constructed as a simple but mechanically stable model of hadrons (Chodos et al., 1974).

D. The mechanical radius of the proton and neutron

The “size” of the proton is commonly defined through the electric charge distribution which is indeed a useful concept, though only for charged hadrons. For an electrically neutral hadron like the neutron, the particle size cannot be inferred in this way. In that case, one may still define an electric mean square charge radius $r_{\text{ch}}^2 = 6 G'_E(0)$ in terms of the derivative of the electric FF $G_E(t)$ at $t = 0$. But for the neutron $r_{\text{ch}}^2 < 0$ which gives insights about the distribution of electric charge inside neutron, but not about its size. This is ultimately due to the neutron’s charge distribution not being positive definite.

The positive-definite normal force per unit area, (49), is an ideal quantity to define the size of the nucleon. One can define the *mechanical radius* as (Polyakov and Schweitzer, 2018a,b)

$$r_{\text{mech}}^2 = \frac{\int d^3r r^2 p_n(r)}{\int d^3r p_n(r)} = \frac{6D(0)}{\int_{-\infty}^0 dt D(t)}. \quad (51)$$

Interestingly, this is an “anti-derivative” of a GFF as compared to the electric mean square charge radius defined in terms of the derivative of the electric FF at $t = 0$. With this definition, the proton and neutron have the same radius (modulo isospin violating effects). Notice also that the (isovector) electric mean square charge radius diverges in the chiral limit and is therefore inadequate to define the proton size in that case, while the mechanical radius in (51) remains finite in the chiral limit (Polyakov and Schweitzer, 2018b). The mechanical radius of the proton is predicted to be somewhat smaller than its charge radius in soliton models (Cebulla et al., 2007; Goeke et al., 2007a). The charge and mechanical radii become equal in the non-relativistic limit which was derived in the bag model (Lorcé et al., 2022b; Neubelt et al., 2020).

E. First visualization of forces from experiment

The first visualization of the force distributions in the proton was presented in (Burkert et al., 2018) which will be reviewed here. As detailed in Sec. IV.B, the DVCS data from JLab experiments (Girod et al., 2008; Jo et al., 2015) provided information on the observable $\mathcal{C}_{\mathcal{H}}(t)$ in (32), from which, under certain reasonable (at

present necessary) assumptions, information about the quark contribution $D_{u+d}(t)$ of the proton was deduced. Based on this information, (48) yields the results for the pressure $p_q(r)$ and the shear force $s_q(r)$ of quarks displayed in Fig. 13 (the index q denotes here $u + d$ quark contributions, with heavier quarks neglected). In order to obtain $p_q(r)$, the additional assumption was made that $\bar{C}_q(t)$ can be neglected.

The $r^2 p_q(r)$ distribution is positive, peaks near 0.25 fm, changes sign near 0.6 fm, and reaches its minimum value

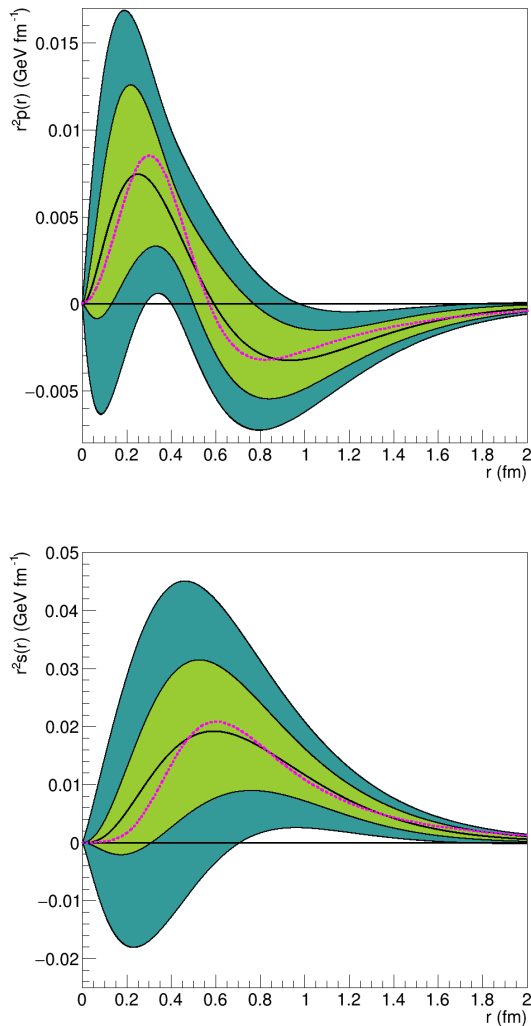


FIG. 13 The distributions of pressure $r^2 p_q(r)$ (top) and shear stress $r^2 s_q(r)$ (bottom) on quarks in the proton based on JLab data (Burkert et al., 2018). The central lines show the best fit. The outer shaded areas mark the uncertainties when only data prior to the CLAS data are included. The inner shaded areas represent the uncertainties when the CLAS data are used. The widths of the bands are dominated by systematic uncertainties [which include extrapolation in unmeasured ξ -region when evaluating (32) and neglect of higher-order terms in the Gegenbauer expansion described in (41)]. The dotted magenta curves represent the model predictions of (Goeke et al., 2007a).

around 1.0 fm. The peak value of $r^2 s_q(r)$ is around 20 MeV fm $^{-1}$, and occurs near 0.6 fm from the proton’s center, where the shear force, given by $4\pi r^2 s_q(r)$, reaches 240 MeV fm $^{-1}$ or 38 kN, an appreciably strong force inside the tiny proton. It is interesting to observe that these results are consistent with predictions from the chiral quark-soliton model (Goeke et al., 2007a) within the (large) systematic uncertainties in the data.

The quark contribution to the normal and tangential forces, $p_{n,q}$ and $p_{t,q}(r)$ as defined in Sec. VI.C, are displayed in a two-dimensional plot in Fig. 14. This figure shows the 3D distributions inside the proton in a slice going through the “equatorial plane”. The normal forces are strongest at mid-distances near 0.5 fm from the proton center and drop towards the center and towards the outer periphery. The tangential forces exhibit a node near 0.40 fm from the center.

F. The D -term and long-range forces

Among the open questions in theory is the issue of how to define the D -term in the presence of long-range forces. It was shown in a classical model of the proton (Bialynicki-Birula, 1993) that $D(t)$ diverges like $1/\sqrt{-t}$ for $t \rightarrow 0$ due to the $\frac{1}{r}$ -behavior of the Coulomb potential (Varma and Schweitzer, 2020). This result is model-independent and was found also for charged pions in chiral perturbation theory (Kubis and Meissner, 2000), in calculations of quantum corrections to the Reissner-Nordström and Kerr-Newman metrics (Donoghue et al., 2002), and for the electron in QED (Metz et al., 2021).

There have been studies of the D -term for the H-atom (Ji and Liu, 2021, 2022), which defy the interpretation presented here. This is perhaps not a surprise considering the differences between hadronic and atomic bound states. Atoms are comparatively large, low-density objects. Pressure concepts from continuum mechanics might not apply to atoms whose stability is well-understood within non-relativistic quantum mechanics. In contrast to this, the proton as a QCD bound state has nearly the same mass as an H-atom but a much smaller size $\sim 10^{-15}$ m and constitutes a compact high-density system (15 orders of magnitude more dense than an atom) where continuum mechanics concepts may be applied and provide insightful interpretations. Another important aspect might be played by the role of confinement absent for atoms which can be easily ionized. Hadrons constitute a much different type of bound state in this respect. More theoretical work is needed to clarify these issues.

The deeper reason why $D(t)$ diverges for $t \rightarrow 0$ due to QED effects might be ultimately related to the presence of a massless physical state (the photon) which has profound consequences in a theory. Notice that $D(t)$ is the only GFF which exhibits this feature when QED ef-

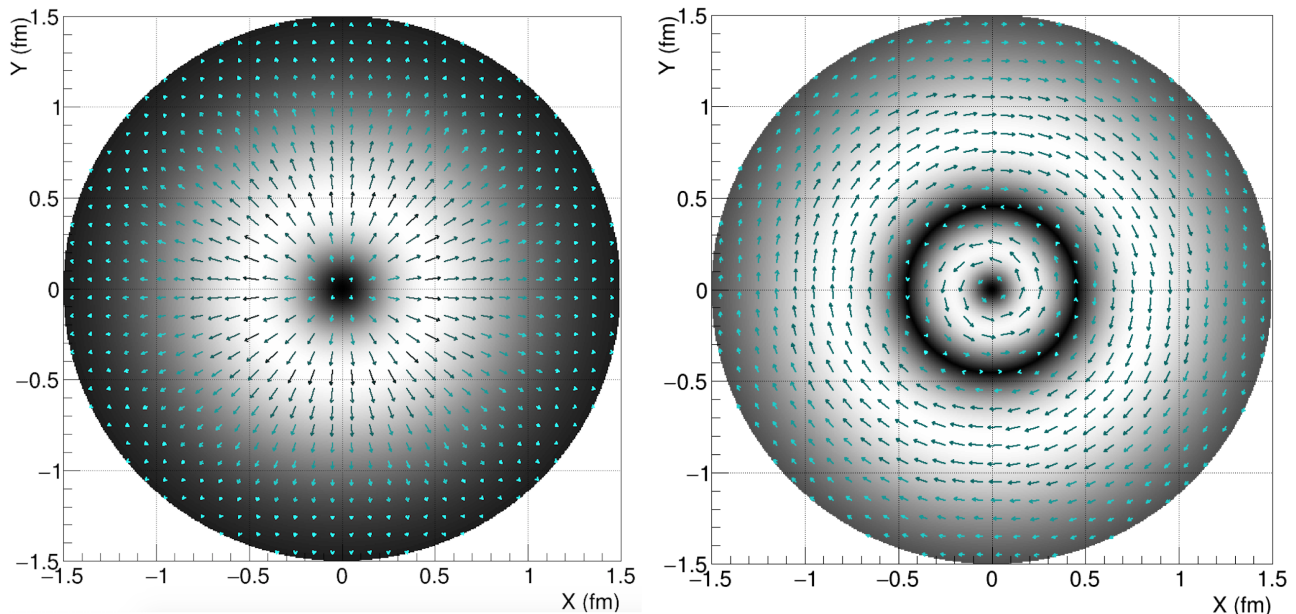


FIG. 14 2D display of the quark contribution to the distribution of forces in the proton as a function of the distance from the proton's center. The light gray shading and longer arrows indicate areas of stronger forces, the dark shading and shorter arrows indicate areas of weaker forces. Left panel: Normal forces as a function of distance from the center. The arrows change magnitude and point always radially outwards. Right panel: Tangential forces as a function of distance from the center. The forces change direction and magnitude as indicated by the direction and lengths of the arrows. They change sign near 0.4 fm from the proton center.

fects are included. There are two reasons for this. First, the other proton GFFs are constrained at $t = 0$, see (6) and (7), while $D(t)$ is not. Second, $D(t)$ is the GFF most sensitive to forces in a system (Hudson and Schweitzer, 2017). Notice that $D(t)$ is multiplied by the prefactor $(\Delta^\mu \Delta^\nu - g^{\mu\nu} \Delta^2)$ such that despite the divergence of $D(t)$ due to QED effects the matrix element $\langle p' | T_a^{\mu\nu} | p \rangle$ is well-behaved in the forward limit.

VII. SUMMARY AND OUTLOOK

This Colloquium gives an overview of the exciting recent developments along a new avenue of experimental and theoretical studies of the gravitational structure of hadrons, especially the proton.

The gravitational form factors of the proton rose to prominence after the works of Xiangdong Ji (Ji, 1995a, 1997b) illustrated how they can be used to gain insight into fundamental questions such as: how much do quarks and gluons contribute to the mass and the spin of the proton? Soon afterwards, Maxim Polyakov (Polyakov, 2003) showed that they also provide information about the spatial distribution of mass and spin, and allow one to study the forces at play in the bound system. These works triggered many follow up studies and investigations which have deepened our understanding of the proton structure.

Through matrix elements of the energy-momentum operator, the gravitational form factors of the proton

and other hadrons have been studied in theoretical approaches including a wide range of models and in numerical calculations in the framework of lattice QCD. In broad terms, the simplest aspects of the EMT structure of the proton and other hadrons (such as the pion) have been understood from theory for some number of years, and first-principles calculations providing complete and controlled decompositions of the proton's mass and spin, for example, are now available. On the other hand, more complicated aspects of proton and nuclear structure, such as gluon gravitational form factors, the x -dependence of generalized parton distributions, and energy-momentum tensor matrix elements in light nuclei, have been computed for the first time in the last several years, as yet without complete systematic control, and significant progress can yet be expected over the next decade. Theory insight into these fundamental aspects of proton and nuclear structure is thus currently in a phase of rapid progress, complementing the improvement of experimental constraints on these quantities and, importantly, providing predictions which inform the target kinematics for future experiments.

The first experimental results, discussed in this colloquium, are based on precise measurements of the deeply virtual Compton scattering process with polarized electron beam, that determined the beam-spin asymmetry and the absolute differential cross section of $ep \rightarrow ep\gamma$. Measurements covered a limited range in the kinematic variables which made it necessary to employ information

from high-energy collider data to constrain the data fit in the region that was not covered in the Jlab experiment. Consequently, large systematic uncertainties were assigned to the results.

New experimental results on deeply virtual Compton scattering measurements with polarized electron beams at higher energy have recently been published from experiments with CLAS12 (Christiaens *et al.*, 2022) and Hall A at Jefferson Laboratory (Georges *et al.*, 2022). They extend the kinematic reach both to higher and to lower values in ξ , and increase the range covered in Q^2 . The latter will allow for more sensitive scaling tests. These new data may also support application of machine learning techniques and artificial neural networks as have been developed by several groups (Berthou *et al.*, 2018; Grigsby *et al.*, 2021; Kumerički, 2019).

Ongoing experiments and future planned measurements that employ polarized proton and deuterium (neutron) targets, have strong sensitivity to Compton form factor \mathcal{E} , which is needed to measure the quark angular momentum distribution $J_q(t)$ in the proton. The plan to extend the Jefferson Lab's electron accelerator energy reach to 22 GeV would more fully open access to employing J/Ψ production near threshold in a wide t range, and some ξ range to access the gluon part $D_G(t)$ of the proton's D -term.

A longer term perspective is provided by the planned Electron-Ion Collider projects in the US (Abdul Khalek *et al.*, 2022; Burkert *et al.*, 2022) and in China (Anderle *et al.*, 2021). The US project will extend the kinematic reach in $x_B > 10^{-4}$ and thus will cover with high operational luminosity up to $10^{34} \text{ cm}^{-2} \text{ s}^{-1}$ the gluon dominated domain. It features polarized electron and polarized proton beams, the latter longitudinally or transversely polarized, and light ion beams. The EIC in China focuses on the lower energy domain $x_B > 10^{-3}$. Both of the colliders complement the fixed-target experiments, which operate dominantly in the valence quark and the $q\bar{q}$ -sea domain at very high luminosity.

Currently available data allow for a first glimpse into this emerging new field of the proton internal structure, complementing what has been learned in many detailed experiments over the past 70 years of experiments and theoretical studies of the proton structure with the first piece of information on the proton's mechanical properties.

This new avenue of research has been rapidly developing theoretically, and the first experimental results on the proton firmly established the study of mechanical properties of sub-atomic particle as an exciting new field of fundamental science. Many objects on earth, in the solar system and in the universe are described by their equation of state, where the internal pressure plays an essential role. Some of these objects are listed in Figure 15. The study discussed in this Colloquium adds the smallest object with the highest internal pressure to this list

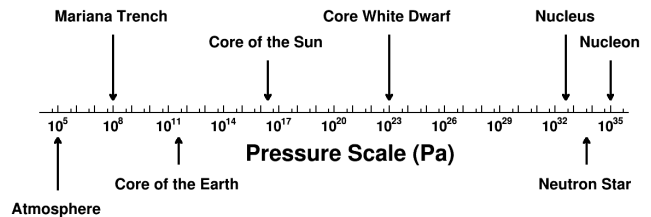


FIG. 15 Comparison of peak pressures inside various objects on earth, in the solar system, and in the universe.

of objects that have been studied so far. The peak pressure inside the proton is approximately 10^{35} Pascal. It tops by 30 orders of magnitude the atmospheric pressure on earth, and even exceeds the pressure in the core of the most densely packed known macroscopic objects in the universe, neutron stars. Other subatomic objects such as pions, kaons, hyperons, and light and heavy nuclei may be subject of experimental investigation in the future. The scientific instruments needed to study them efficiently are in preparation.

The gravitational form factors provide the key to address fundamental questions about the mass, spin, and internal forces inside the proton and other hadrons. Theoretical, experimental and phenomenological studies of gravitational form factors provide exciting insights. In this emerging new field, there are many inspiring lessons to learn and there is much to look forward to.

ACKNOWLEDGMENTS

The authors cannot mention the names of all colleagues and acknowledge all discussions during and prior to the preparation of this Colloquium. We wish to name only Maxim Polyakov who until his untimely death in August 2021 influenced or initiated many of the reviewed topics. Special thanks go to Joanna Griffin for professional assistance with preparing diagrams and figures. This material is based upon work supported by the U.S. Department of Energy, Office of Science, Office of Nuclear Physics under contract DE-AC05-06OR23177. P. Schweitzer was supported by the NSF grant under the Contract No. 2111490. P. Shanahan was supported in part by the U.S. Department of Energy, Office of Science, Office of Nuclear Physics, under grant Contract Number DE-SC0011090 and by Early Career Award DE-SC0021006, by a NEC research award, and by the Carl G and Shirley Sontheimer Research Fund.

ACRONYMS

A heavy use of acronyms can make a text difficult to read for readers not familiar with the field, while no use

of acronyms can make it unreadable for those who are familiar. The authors found it indispensable to introduce a number of acronyms which are explained at their first occurrence and are collected here for convenience.

<i>AM</i>	angular momentum
<i>BSA</i>	beam spin asymmetry
<i>CFE</i>	Compton form factor
<i>DIS</i>	deep inelastic scattering
<i>DVCS</i>	deeply virtual Compton scattering
<i>DDVCS</i>	double deeply virtual Compton scattering
<i>EIC</i>	Electron-Ion Collider
<i>EMT</i>	energy momentum tensor
<i>FF</i>	form factor
<i>GDA</i>	generalized distribution amplitude
<i>GFF</i>	gravitational form factor
<i>GPD</i>	generalized parton distribution
<i>JLab</i>	Jefferson Lab
<i>PDF</i>	parton distribution function
<i>QCD</i>	quantum chromodynamics
<i>QED</i>	quantum electrodynamics
<i>TCS</i>	time-like Compton scattering

REFERENCES

- Abbott, D, et al. (PEPPo) (2016), “Production of Highly Polarized Positrons Using Polarized Electrons at MeV Energies,” *Phys. Rev. Lett.* **116** (21), 214801, [arXiv:1606.08877 \[physics.acc-ph\]](#).
- Abdul Khalek, R, et al. (2022), “Science Requirements and Detector Concepts for the Electron-Ion Collider: EIC Yellow Report,” *Nucl. Phys. A* **1026**, 122447, [arXiv:2103.05419 \[physics.ins-det\]](#).
- Abidin, Zainul, and Carl E. Carlson (2008), “Gravitational Form Factors in the Axial Sector from an AdS/QCD Model,” *Phys. Rev. D* **77**, 115021, [arXiv:0804.0214 \[hep-ph\]](#).
- Abidin, Zainul, and Carl E. Carlson (2009), “Nucleon electromagnetic and gravitational form factors from holography,” *Phys. Rev. D* **79**, 115003, [arXiv:0903.4818 \[hep-ph\]](#).
- Adloff, C, et al. (H1) (2001), “Measurement of deeply virtual Compton scattering at HERA,” *Phys. Lett. B* **517**, 47–58, [arXiv:hep-ex/0107005](#).
- Ahmed, Taushif, Long Chen, and Michał Czakon (2022), “A note on quark and gluon energy-momentum tensors,” [arXiv:2208.01441 \[hep-ph\]](#).
- Aidala, Christine A, Steven D. Bass, Delia Hasch, and Gerhard K. Mallot (2013), “The Spin Structure of the Nucleon,” *Rev. Mod. Phys.* **85**, 655–691, [arXiv:1209.2803 \[hep-ph\]](#).
- Airapetian, A, et al. (HERMES) (2001), “Measurement of the beam spin azimuthal asymmetry associated with deeply virtual Compton scattering,” *Phys. Rev. Lett.* **87**, 182001, [arXiv:hep-ex/0106068](#).
- Airapetian, A, et al. (HERMES) (2011), “Measurement of double-spin asymmetries associated with deeply virtual Compton scattering on a transversely polarized hydrogen target,” *Phys. Lett. B* **704**, 15–23, [arXiv:1106.2990 \[hep-ex\]](#).
- Akhunzyanov, R, et al. (COMPASS) (2019), “Transverse ex-
- tension of partons in the proton probed in the sea-quark range by measuring the DVCS cross section,” *Phys. Lett. B* **793**, 188–194, [Erratum: *Phys.Lett.B* 800, 135129 (2020)], [arXiv:1802.02739 \[hep-ex\]](#).
- Alexandrou, C, S. Bacchio, M. Constantinou, J. Finkenrath, K. Hadjiyiannakou, K. Jansen, G. Koutsou, H. Panagopoulos, and G. Spanoudes (2020a), “Complete flavor decomposition of the spin and momentum fraction of the proton using lattice QCD simulations at physical pion mass,” *Phys. Rev. D* **101** (9), 094513, [arXiv:2003.08486 \[hep-lat\]](#).
- Alexandrou, C, S. Bacchio, M. Constantinou, J. Finkenrath, K. Hadjiyiannakou, K. Jansen, G. Koutsou, and A. Vaquero Aviles-Casco (2020b), “Nucleon axial, tensor, and scalar charges and σ -terms in lattice QCD,” *Phys. Rev. D* **102** (5), 054517, [arXiv:1909.00485 \[hep-lat\]](#).
- Alexandrou, C, M. Constantinou, K. Hadjiyiannakou, K. Jansen, C. Kallidonis, G. Koutsou, A. Vaquero Avilés-Casco, and C. Wiese (2017), “Nucleon Spin and Momentum Decomposition Using Lattice QCD Simulations,” *Phys. Rev. Lett.* **119** (14), 142002, [arXiv:1706.02973 \[hep-lat\]](#).
- Alexandrou, C, et al. (2020c), “Moments of nucleon generalized parton distributions from lattice QCD simulations at physical pion mass,” *Phys. Rev. D* **101** (3), 034519, [arXiv:1908.10706 \[hep-lat\]](#).
- Alexandrou, Constantia, Krzysztof Cichy, Martha Constantinou, Kyriakos Hadjiyiannakou, Karl Jansen, Aurora Scapellato, and Fernanda Steffens (2020d), “Unpolarized and helicity generalized parton distributions of the proton within lattice QCD,” *Phys. Rev. Lett.* **125** (26), 262001, [arXiv:2008.10573 \[hep-lat\]](#).
- Alexandrou, Constantia, Krzysztof Cichy, Martha Constantinou, Kyriakos Hadjiyiannakou, Karl Jansen, Aurora Scapellato, and Fernanda Steffens (2022), “Transversity GPDs of the proton from lattice QCD,” *Phys. Rev. D* **105** (3), 034501, [arXiv:2108.10789 \[hep-lat\]](#).
- Alexandrou, Constantia, Martha Constantinou, Kyriakos Hadjiyiannakou, Karl Jansen, Christos Kallidonis, Giannis Koutsou, and Alejandro Vaquero Avilés-Casco (2018), “Nucleon spin structure from lattice QCD,” *PoS DIS2018*, 148, [arXiv:1807.11214 \[hep-lat\]](#).
- Alharazin, H, D. Djukanovic, J. Gegelia, and M. V. Polyakov (2020), “Chiral theory of nucleons and pions in the presence of an external gravitational field,” *Phys. Rev. D* **102** (7), 076023, [arXiv:2006.05890 \[hep-ph\]](#).
- Alharazin, H, E. Epelbaum, J. Gegelia, U. G. Meißner, and B. D. Sun (2022), “Gravitational form factors of the delta resonance in chiral EFT,” *Eur. Phys. J. C* **82** (10), 907, [arXiv:2209.01233 \[hep-ph\]](#).
- Ali, A, et al. (GlueX) (2019), “First Measurement of Near-Threshold J/ψ Exclusive Photoproduction off the Proton,” *Phys. Rev. Lett.* **123** (7), 072001, [arXiv:1905.10811 \[nucl-ex\]](#).
- Aliev, T M, K. Şimşek, and T. Barakat (2021), “Gravitational formfactors of the ρ , π , and K mesons in the light-cone QCD sum rules,” *Phys. Rev. D* **103**, 054001, [arXiv:2009.07926 \[hep-ph\]](#).
- Alvarez, Luis W, and F. Bloch (1940), “A Quantitative Determination of the Neutron Moment in Absolute Nuclear Magnetons,” *Phys. Rev.* **57**, 111–122.
- Anderle, Daniele P, et al. (2021), “Electron-ion collider in China,” *Front. Phys. (Beijing)* **16** (6), 64701, [arXiv:2102.09222 \[nucl-ex\]](#).
- Anikin, I V (2019), “Gravitational form factors within light-

- cone sum rules at leading order,” *Phys. Rev. D* **99** (9), 094026, [arXiv:1902.00094 \[hep-ph\]](#).
- Anikin, I V, and O. V. Teryaev (2008), “Dispersion relations and QCD factorization in hard reactions,” *Fizika B* **17**, 151–158, [arXiv:0710.4211 \[hep-ph\]](#).
- Arrington, J, et al. (2022), “Physics with CEBAF at 12 GeV and future opportunities,” *Prog. Part. Nucl. Phys.* **127**, 103985, [arXiv:2112.00060 \[nucl-ex\]](#).
- Azizi, K, and U. Özdem (2020), “Nucleon’s energy–momentum tensor form factors in light-cone QCD,” *Eur. Phys. J. C* **80** (2), 104, [arXiv:1908.06143 \[hep-ph\]](#).
- Azizi, K, and U. Özdem (2021), “Gravitational form factors of N(1535) in QCD,” *Nucl. Phys. A* **1015**, 122296, [arXiv:2012.06895 \[hep-ph\]](#).
- Bakker, B L G, E. Leader, and T. L. Trueman (2004), “A Critique of the angular momentum sum rules and a new angular momentum sum rule,” *Phys. Rev. D* **70**, 114001, [arXiv:hep-ph/0406139](#).
- Bali, Gunnar, Sara Collins, Meinulf Göckeler, Rudolf Rödl, Andreas Schäfer, and Andre Sternbeck (2016), “Nucleon generalized form factors from lattice QCD with nearly physical quark masses,” *PoS LATTICE2015*, 118, [arXiv:1601.04818 \[hep-lat\]](#).
- Belinfante, Frederik J (1962), “Consequences of the Postulate of a Complete Commuting Set of Observables in Quantum Electrodynamics,” *Phys. Rev.* **128**, 2832–2837.
- Belitsky, Andrei V, and X. Ji (2002), “Chiral structure of nucleon gravitational form-factors,” *Phys. Lett. B* **538**, 289–297, [arXiv:hep-ph/0203276](#).
- Belitsky, Andrei V, Dieter Mueller, and A. Kirchner (2002), “Theory of deeply virtual Compton scattering on the nucleon,” *Nucl. Phys. B* **629**, 323–392, [arXiv:hep-ph/0112108](#).
- Berger, Edgar R, M. Diehl, and B. Pire (2002), “Time - like Compton scattering: Exclusive photoproduction of lepton pairs,” *Eur. Phys. J. C* **23**, 675–689, [arXiv:hep-ph/0110062](#).
- Berthou, B, et al. (2018), “PARTONS: PARTonic Tomography Of Nucleon Software: A computing framework for the phenomenology of Generalized Parton Distributions,” *Eur. Phys. J. C* **78** (6), 478, [arXiv:1512.06174 \[hep-ph\]](#).
- Bertone, V, H. Dutriex, C. Mezrag, H. Moutarde, and P. Sznajder (2021), “Deconvolution problem of deeply virtual Compton scattering,” *Phys. Rev. D* **103** (11), 114019, [arXiv:2104.03836 \[hep-ph\]](#).
- Białynicki-Birula, Iwo (1993), “Simple relativistic model of a finite size particle,” *Phys. Lett. A* **182**, 346–352, [arXiv:nucl-th/9306006](#).
- Bjorken, J D (1969), “Asymptotic Sum Rules at Infinite Momentum,” *Phys. Rev.* **179**, 1547–1553.
- Bloom, Elliott D, et al. (1969), “High-Energy Inelastic e p Scattering at 6-Degrees and 10-Degrees,” *Phys. Rev. Lett.* **23**, 930–934.
- Boussarie, R, B. Pire, L. Szymanowski, and S. Wallon (2017), “Exclusive photoproduction of a $\gamma\rho$ pair with a large invariant mass,” *JHEP* **02**, 054, [Erratum: *JHEP* 10, 029 (2018)], [arXiv:1609.03830 \[hep-ph\]](#).
- Brandelik, R, et al. (TASSO) (1980), “Evidence for a Spin One Gluon in Three Jet Events,” *Phys. Lett. B* **97**, 453–458.
- Brodsky, Stanley J, Dae Sung Hwang, Bo-Qiang Ma, and Ivan Schmidt (2001), “Light cone representation of the spin and orbital angular momentum of relativistic composite systems,” *Nucl. Phys. B* **593**, 311–335, [arXiv:hep-th/0003082](#).
- Brodsky, Stanley J, and Guy F. de Teramond (2008), “Light-Front Dynamics and AdS/QCD Correspondence: Gravitational Form Factors of Composite Hadrons,” *Phys. Rev. D* **78**, 025032, [arXiv:0804.0452 \[hep-ph\]](#).
- Brommel, D, M. Diehl, M. Gockeler, Ph. Hagler, R. Horsley, D. Pleiter, Paul E. L. Rakow, A. Schafer, G. Schierholz, and J. M. Zanotti (2006), “Structure of the pion from full lattice QCD,” *PoS LAT2005*, 360, [arXiv:hep-lat/0509133](#).
- Brommel, Dirk (2007), *Pion Structure from the Lattice*, Ph.D. thesis (Regensburg U.).
- Burkardt, Matthias (2000), “Impact parameter dependent parton distributions and off forward parton distributions for $\zeta \rightarrow 0$,” *Phys. Rev. D* **62**, 071503, [Erratum: *Phys.Rev.D* 66, 119903 (2002)], [arXiv:hep-ph/0005108](#).
- Burkert, V, et al. (CLAS) (2021), “Beam charge asymmetries for deeply virtual Compton scattering off the proton,” *Eur. Phys. J. A* **57** (6), 186, [arXiv:2103.12651 \[nucl-ex\]](#).
- Burkert, V, et al. (2022), “Precision Studies of QCD in the Low Energy Domain of the EIC,” [arXiv:2211.15746 \[nucl-ex\]](#).
- Burkert, V D, L. Elouadrhiri, and F. X. Girod (2018), “The pressure distribution inside the proton,” *Nature* **557** (7705), 396–399.
- Burkert, V D, et al. (2020), “The CLAS12 Spectrometer at Jefferson Laboratory,” *Nucl. Instrum. Meth. A* **959**, 163419.
- Camacho, C Muñoz, et al. (Jefferson Lab Hall A, Hall A DVCS) (2006), “Scaling tests of the cross-section for deeply virtual compton scattering,” *Phys. Rev. Lett.* **97**, 262002, [arXiv:nucl-ex/0607029](#).
- Cantara, Michael, Manuel Mai, and Peter Schweitzer (2016), “The energy-momentum tensor and D-term of Q-clouds,” *Nucl. Phys. A* **953**, 1–20, [arXiv:1510.08015 \[hep-ph\]](#).
- Cebulla, C, K. Goeke, J. Ossmann, and P. Schweitzer (2007), “The Nucleon form-factors of the energy momentum tensor in the Skyrme model,” *Nucl. Phys. A* **794**, 87–114, [arXiv:hep-ph/0703025](#).
- Chadwick, J (1932), “Possible Existence of a Neutron,” *Nature* **129**, 312.
- Chakrabarti, Dipankar, Chandan Mondal, and Asmita Mukherjee (2015), “Gravitational form factors and transverse spin sum rule in a light front quark-diquark model in AdS/QCD,” *Phys. Rev. D* **91** (11), 114026, [arXiv:1505.02013 \[hep-ph\]](#).
- Chakrabarti, Dipankar, Chandan Mondal, Asmita Mukherjee, Sreeraj Nair, and Xingbo Zhao (2020), “Gravitational form factors and mechanical properties of proton in a light-front quark-diquark model,” *Phys. Rev. D* **102**, 113011, [arXiv:2010.04215 \[hep-ph\]](#).
- Chambers, A J, R. Horsley, Y. Nakamura, H. Perlt, P. E. L. Rakow, G. Schierholz, A. Schiller, K. Somfleth, R. D. Young, and J. M. Zanotti (2017), “Nucleon Structure Functions from Operator Product Expansion on the Lattice,” *Phys. Rev. Lett.* **118** (24), 242001, [arXiv:1703.01153 \[hep-lat\]](#).
- Chatagnon, P, et al. (CLAS) (2021), “First Measurement of Timelike Compton Scattering,” *Phys. Rev. Lett.* **127** (26), 262501, [arXiv:2108.11746 \[hep-ex\]](#).
- Chekanov, S, et al. (ZEUS) (2003), “Measurement of deeply virtual Compton scattering at HERA,” *Phys. Lett. B* **573**, 46–62, [arXiv:hep-ex/0305028](#).
- Chen, J P, H. Gao, T. K. Hemmick, Z. E. Meziani, and P. A. Souder (SoLID) (2014), “A White Paper on SoLID

- (Solenoidal Large Intensity Device),” [arXiv:1409.7741 \[nucl-ex\]](#).
- Chen, S, et al. (CLAS) (2006), “Measurement of deeply virtual compton scattering with a polarized proton target,” *Phys. Rev. Lett.* **97**, 072002, [arXiv:hep-ex/0605012](#).
- Chen, Xiang-Song, Xiao-Fu Lu, Wei-Min Sun, Fan Wang, and T. Goldman (2008), “Spin and orbital angular momentum in gauge theories: Nucleon spin structure and multipole radiation revisited,” *Phys. Rev. Lett.* **100**, 232002, [arXiv:0806.3166 \[hep-ph\]](#).
- Chodos, A, R. L. Jaffe, K. Johnson, Charles B. Thorn, and V. F. Weisskopf (1974), “A New Extended Model of Hadrons,” *Phys. Rev. D* **9**, 3471–3495.
- Choudhary, Poonam, Bheemsehan Gurjar, Dipankar Chakrabarti, and Asmita Mukherjee (2022), “Gravitational form factors and mechanical properties of the proton: Connections between distributions in 2D and 3D,” *Phys. Rev. D* **106** (7), 076004, [arXiv:2206.12206 \[hep-ph\]](#).
- Christiaens, G, et al. (CLAS) (2022), “First CLAS12 measurement of DVCS beam-spin asymmetries in the extended valence region,” [arXiv:2211.11274 \[hep-ex\]](#).
- Collins, John C, Anthony Duncan, and Satish D. Joglekar (1977), “Trace and Dilatation Anomalies in Gauge Theories,” *Phys. Rev. D* **16**, 438–449.
- Collins, John C, and Andreas Freund (1999), “Proof of factorization for deeply virtual Compton scattering in QCD,” *Phys. Rev. D* **59**, 074009, [arXiv:hep-ph/9801262](#).
- Constantinou, Martha, et al. (2021), “Parton distributions and lattice-QCD calculations: Toward 3D structure,” *Prog. Part. Nucl. Phys.* **121**, 103908, [arXiv:2006.08636 \[hep-ph\]](#).
- Cosyn, Wim, Sabrina Cotogno, Adam Freese, and Cédric Lorcé (2019), “The energy-momentum tensor of spin-1 hadrons: formalism,” *Eur. Phys. J. C* **79** (6), 476, [arXiv:1903.00408 \[hep-ph\]](#).
- Cotogno, Sabrina, Cédric Lorcé, and Peter Lowdon (2019), “Poincaré constraints on the gravitational form factors for massive states with arbitrary spin,” *Phys. Rev. D* **100** (4), 045003, [arXiv:1905.11969 \[hep-th\]](#).
- Cotogno, Sabrina, Cédric Lorcé, Peter Lowdon, and Manuel Morales (2020), “Covariant multipole expansion of local currents for massive states of any spin,” *Phys. Rev. D* **101** (5), 056016, [arXiv:1912.08749 \[hep-ph\]](#).
- Dashen, Roger F, Elizabeth Ellen Jenkins, and Aneesh V. Manohar (1994), “The $1/N_c$ expansion for baryons,” *Phys. Rev. D* **49**, 4713, [Erratum: *Phys.Rev.D* 51, 2489 (1995)], [arXiv:hep-ph/9310379](#).
- Detmold, W, D. Pefkou, and P. E. Shanahan (2017), “Off-forward gluonic structure of vector mesons,” *Phys. Rev. D* **95** (11), 114515, [arXiv:1703.08220 \[hep-lat\]](#).
- Detmold, William, Anthony V. Grebe, Issaku Kanamori, C. J. David Lin, Robert J. Perry, and Yong Zhao (HOPE) (2021a), “Parton physics from a heavy-quark operator product expansion: Formalism and Wilson coefficients,” *Phys. Rev. D* **104** (7), 074511, [arXiv:2103.09529 \[hep-lat\]](#).
- Detmold, William, Marc Illa, David J. Murphy, Patrick Oare, Kostas Orginos, Phiala E. Shanahan, Michael L. Wagman, and Frank Winter (NPLQCD) (2021b), “Lattice QCD Constraints on the Parton Distribution Functions of ^3He ,” *Phys. Rev. Lett.* **126** (20), 202001, [arXiv:2009.05522 \[hep-lat\]](#).
- Detmold, William, and C. J. David Lin (2006), “Deep-inelastic scattering and the operator product expansion in lattice QCD,” *Phys. Rev. D* **73**, 014501, [arXiv:hep-lat/0507007](#).
- Diehl, M, T. Gousset, B. Pire, and O. Teryaev (1998), “Probing partonic structure in $\gamma^*\gamma \rightarrow \pi\pi$ near threshold,” *Phys. Rev. Lett.* **81**, 1782–1785, [arXiv:hep-ph/9805380](#).
- Diehl, M, and D. Yu. Ivanov (2007), “Dispersion representations for hard exclusive processes: beyond the Born approximation,” *Eur. Phys. J. C* **52**, 919–932, [arXiv:0707.0351 \[hep-ph\]](#).
- Diehl, M, A. Manashov, and A. Schafer (2006), “Chiral perturbation theory for nucleon generalized parton distributions,” *Eur. Phys. J. A* **29**, 315–326, [Erratum: *Eur.Phys.J.A* 56, 220 (2020)], [arXiv:hep-ph/0608113](#).
- Donoghue, J F, E. Golowich, and Barry R. Holstein (2014), [Dynamics of the standard model](#), Vol. 2 (CUP).
- Donoghue, John F, J. Gasser, and H. Leutwyler (1990), “The Decay of a Light Higgs Boson,” *Nucl. Phys. B* **343**, 341–368.
- Donoghue, John F, Barry R. Holstein, Björn Garbrecht, and Thomas Konstandin (2002), “Quantum corrections to the Reissner-Nordström and Kerr-Newman metrics,” *Phys. Lett. B* **529**, 132–142, [Erratum: *Phys.Lett.B* 612, 311–312 (2005)], [arXiv:hep-th/0112237](#).
- Donoghue, John F, and H. Leutwyler (1991), “Energy and momentum in chiral theories,” *Z. Phys. C* **52**, 343–351.
- Duplanić, G, K. Passek-Kumerički, B. Pire, L. Szymanowski, and S. Wallon (2018), “Probing axial quark generalized parton distributions through exclusive photoproduction of a $\gamma\pi^\pm$ pair with a large invariant mass,” *JHEP* **11**, 179, [arXiv:1809.08104 \[hep-ph\]](#).
- Dutrieux, H, C. Lorcé, H. Moutarde, P. Sznajder, A. Trawiński, and J. Wagner (2021), “Phenomenological assessment of proton mechanical properties from deeply virtual Compton scattering,” *Eur. Phys. J. C* **81** (4), 300, [arXiv:2101.03855 \[hep-ph\]](#).
- Engelhardt, M, J. R. Green, N. Hasan, S. Krieg, S. Meinel, J. Negele, A. Pochinsky, and S. Syritsyn (2020), “From Ji to Jaffe-Manohar orbital angular momentum in lattice QCD using a direct derivative method,” *Phys. Rev. D* **102** (7), 074505, [arXiv:2008.03660 \[hep-lat\]](#).
- Epelbaum, E, J. Gegelia, U. G. Meißner, and M. V. Polyakov (2022), “Chiral theory of ρ -meson gravitational form factors,” *Phys. Rev. D* **105** (1), 016018, [arXiv:2109.10826 \[hep-ph\]](#).
- Feynman, Richard P (1969), “Very high-energy collisions of hadrons,” *Phys. Rev. Lett.* **23**, 1415–1417, [494(1969)].
- Fiore, Roberto, Laszlo Jenkovszky, and Maryna Oleksiienko (2021), “On matter and pressure distribution in nucleons,” [arXiv:2112.00605 \[hep-ph\]](#).
- Freese, Adam, and Wim Cosyn (2022a), “Spatial densities of momentum and forces in spin-one hadrons,” [arXiv:2207.10787 \[hep-ph\]](#).
- Freese, Adam, and Wim Cosyn (2022b), “Spatial densities of the photon on the light front,” [arXiv:2207.10788 \[hep-ph\]](#).
- Freese, Adam, Adam Freese, Ian C. Cloët, and Ian C. Cloët (2019), “Gravitational form factors of light mesons,” *Phys. Rev. C* **100** (1), 015201, [Erratum: *Phys.Rev.C* 105, 059901 (2022)], [arXiv:1903.09222 \[nucl-th\]](#).
- Freese, Adam, and Gerald A. Miller (2021), “Forces within hadrons on the light front,” *Phys. Rev. D* **103**, 094023, [arXiv:2102.01683 \[hep-ph\]](#).
- Freese, Adam, and Gerald A. Miller (2022), “Unified formalism for electromagnetic and gravitational probes: Densities,” *Phys. Rev. D* **105** (1), 014003, [arXiv:2108.03301 \[hep-ph\]](#).
- Friot, S, B. Pire, and L. Szymanowski (2007), “Deeply virtual

- compton scattering on a photon and generalized parton distributions in the photon,” *Phys. Lett. B* **645**, 153–160, [arXiv:hep-ph/0611176](#).
- Frisch, Robert, and Otto Stern (1933), “Über die magnetische Ablenkung von Wasserstoffmolekülen und das magnetische Moment des Protons,” *Z. Phys.* **85**, 4–16.
- Fu, Dongyan, Bao-Dong Sun, and Yubing Dong (2022), “Electromagnetic and gravitational form factors of Δ resonance in a covariant quark-diquark approach,” *Phys. Rev. D* **105** (9), 096002, [arXiv:2201.08059 \[hep-ph\]](#).
- Fujita, Mitsutoshi, Yoshitaka Hatta, Shigeki Sugimoto, and Takahiro Ueda (2022), “Nucleon D-term in holographic quantum chromodynamics,” *PTEP* **2022** (9), 093B06, [arXiv:2206.06578 \[hep-th\]](#).
- Gabdrakhmanov, I R, and O. V. Teryaev (2012), “Analyticity and sum rules for photon GPDs,” *Phys. Lett. B* **716**, 417–424, [arXiv:1204.6471 \[hep-ph\]](#).
- Gegelia, Jambul, and Maxim V. Polyakov (2021), “A bound on the nucleon Druck-term from chiral EFT in curved space-time and mechanical stability conditions,” *Phys. Lett. B* **820**, 136572, [arXiv:2104.13954 \[hep-ph\]](#).
- Gell-Mann, Murray (1964), “A Schematic Model of Baryons and Mesons,” *Phys. Lett.* **8**, 214–215.
- Georges, F, et al. (Jefferson Lab Hall A) (2022), “Deeply Virtual Compton Scattering Cross Section at High Bjorken x_B ,” *Phys. Rev. Lett.* **128** (25), 252002, [arXiv:2201.03714 \[hep-ph\]](#).
- Ghim, Nam-Yong, Hyun-Chul Kim, Ulugbek Yakhshiev, and Ghil-Seok Yang (2022), “Medium modification of singly heavy baryons in a pion-mean field approach,” [arXiv:2211.04277 \[hep-ph\]](#).
- Girod, F X, et al. (CLAS) (2008), “Measurement of Deeply virtual Compton scattering beam-spin asymmetries,” *Phys. Rev. Lett.* **100**, 162002, [arXiv:0711.4805 \[hep-ex\]](#).
- Goeke, K, J. Grabis, J. Ossmann, M. V. Polyakov, P. Schweitzer, A. Silva, and D. Urbano (2007a), “Nucleon form-factors of the energy momentum tensor in the chiral quark-soliton model,” *Phys. Rev. D* **75**, 094021, [arXiv:hep-ph/0702030](#).
- Goeke, K, J. Grabis, J. Ossmann, P. Schweitzer, A. Silva, and D. Urbano (2007b), “The pion mass dependence of the nucleon form-factors of the energy momentum tensor in the chiral quark-soliton model,” *Phys. Rev. C* **75**, 055207, [arXiv:hep-ph/0702031](#).
- Goeke, K, Maxim V. Polyakov, and M. Vanderhaeghen (2001), “Hard exclusive reactions and the structure of hadrons,” *Prog. Part. Nucl. Phys.* **47**, 401–515, [arXiv:hep-ph/0106012](#).
- Grigsby, Jake, Brandon Kriesten, Joshua Hoskins, Simonetta Liuti, Peter Alonzi, and Matthias Burkardt (2021), “Deep learning analysis of deeply virtual exclusive photoproduction,” *Phys. Rev. D* **104** (1), 016001, [arXiv:2012.04801 \[hep-ph\]](#).
- Grocholski, Oskar, Bernard Pire, Paweł Sznajder, Lech Szymanowski, and Jakob Wagner (2022), “Phenomenology of diphoton photoproduction at next-to-leading order,” *Phys. Rev. D* **105** (9), 094025, [arXiv:2204.00396 \[hep-ph\]](#).
- Gross, David J, and Frank Wilczek (1973), “Ultraviolet Behavior of Nonabelian Gauge Theories,” *Phys. Rev. Lett.* **30**, 1343–1346, [271(1973)].
- Guo, Yuxun, Xiangdong Ji, and Yizhuang Liu (2021), “QCD Analysis of Near-Threshold Photon-Proton Production of Heavy Quarkonium,” *Phys. Rev. D* **103** (9), 096010, [arXiv:2103.11506 \[hep-ph\]](#).
- Guzey, V, and M. Siddikov (2006), “On the A-dependence of nuclear generalized parton distributions,” *J. Phys. G* **32**, 251–268, [arXiv:hep-ph/0509158](#).
- Hagler, Ph, et al. (LHPC) (2008), “Nucleon Generalized Parton Distributions from Full Lattice QCD,” *Phys. Rev. D* **77**, 094502, [arXiv:0705.4295 \[hep-lat\]](#).
- Hatta, Yoshitaka (2012), “Notes on the orbital angular momentum of quarks in the nucleon,” *Phys. Lett. B* **708**, 186–190, [arXiv:1111.3547 \[hep-ph\]](#).
- Hatta, Yoshitaka, Abha Rajan, and Kazuhiro Tanaka (2018), “Quark and gluon contributions to the QCD trace anomaly,” *JHEP* **12**, 008, [arXiv:1810.05116 \[hep-ph\]](#).
- Hatta, Yoshitaka, and Mark Strikman (2021), “ ϕ -meson lepto-production near threshold and the strangeness D-term,” *Phys. Lett. B* **817**, 136295, [arXiv:2102.12631 \[hep-ph\]](#).
- Heisenberg, W (1932), “On the structure of atomic nuclei,” *Z. Phys.* **77**, 1–11.
- Hoferichter, Martin, Jacobo Ruiz de Elvira, Bastian Kubis, and Ulf-G. Meißner (2016), “Roy–Steiner-equation analysis of pion–nucleon scattering,” *Phys. Rept.* **625**, 1–88, [arXiv:1510.06039 \[hep-ph\]](#).
- ’t Hooft, Gerard, and M. J. G. Veltman (1972), “Regularization and Renormalization of Gauge Fields,” *Nucl. Phys. B* **44**, 189–213.
- Horn, Tanja, and Craig D. Roberts (2016), “The pion: an enigma within the Standard Model,” *J. Phys. G* **43** (7), 073001, [arXiv:1602.04016 \[nucl-th\]](#).
- Hudson, Jonathan, and Peter Schweitzer (2017), “D term and the structure of pointlike and composed spin-0 particles,” *Phys. Rev. D* **96** (11), 114013, [arXiv:1712.05316 \[hep-ph\]](#).
- Hwang, D S, and Dieter Mueller (2008), “Implication of the overlap representation for modelling generalized parton distributions,” *Phys. Lett. B* **660**, 350–359, [arXiv:0710.1567 \[hep-ph\]](#).
- Ivanov, D Yu, B. Pire, L. Szymanowski, and O. V. Teryaev (2002), “Probing chiral odd GPD’s in diffractive electroproduction of two vector mesons,” *Phys. Lett. B* **550**, 65–76, [arXiv:hep-ph/0209300](#).
- Ivanov, D Yu, A. Schafer, L. Szymanowski, and G. Krasnikov (2004), “Exclusive photoproduction of a heavy vector meson in QCD,” *Eur. Phys. J. C* **34** (3), 297–316, [Erratum: *Eur.Phys.J.C* 75, 75 (2015)], [arXiv:hep-ph/0401131](#).
- Jaffe, R L, and Aneesh Manohar (1990), “The G(1) Problem: Fact and Fantasy on the Spin of the Proton,” *Nucl. Phys. B* **337**, 509–546.
- Ji, Xiang-Dong (1995a), “A QCD analysis of the mass structure of the nucleon,” *Phys. Rev. Lett.* **74**, 1071–1074, [arXiv:hep-ph/9410274](#).
- Ji, Xiang-Dong (1995b), “Breakup of hadron masses and energy - momentum tensor of QCD,” *Phys. Rev. D* **52**, 271–281, [arXiv:hep-ph/9502213](#).
- Ji, Xiang-Dong (1997a), “Deeply virtual Compton scattering,” *Phys. Rev. D* **55**, 7114–7125, [arXiv:hep-ph/9609381](#).
- Ji, Xiang-Dong (1997b), “Gauge-Invariant Decomposition of Nucleon Spin,” *Phys. Rev. Lett.* **78**, 610–613, [arXiv:hep-ph/9603249](#).
- Ji, Xiang-Dong (1998), “Lorentz symmetry and the internal structure of the nucleon,” *Phys. Rev. D* **58**, 056003, [arXiv:hep-ph/9710290](#).
- Ji, Xiang-Dong, W. Melnitchouk, and X. Song (1997), “A Study of off forward parton distributions,” *Phys. Rev. D* **56**, 5511–5523, [arXiv:hep-ph/9702379](#).

- Ji, Xiangdong (2013), “Parton physics on a euclidean lattice,” *Phys. Rev. Lett.* **110**, 262002.
- Ji, Xiangdong (2021), “Proton mass decomposition: naturalness and interpretations,” *Front. Phys. (Beijing)* **16** (6), 64601, [arXiv:2102.07830 \[hep-ph\]](#).
- Ji, Xiangdong, and Yizhuang Liu (2021), “Momentum-Current Gravitational Multipoles of Hadrons,” [arXiv:2110.14781](#).
- Ji, Xiangdong, and Yizhuang Liu (2022), “Gravitational Tensor-Monopole Moment of Hydrogen Atom To Order $\mathcal{O}(\alpha)$,” [arXiv:2208.05029 \[hep-ph\]](#).
- Ji, Xiangdong, Feng Yuan, and Yong Zhao (2021), “What we know and what we don’t know about the proton spin after 30 years,” *Nature Rev. Phys.* **3** (1), 27–38, [arXiv:2009.01291 \[hep-ph\]](#).
- Jo, H S, et al. (CLAS) (2015), “Cross sections for the exclusive photon electroproduction on the proton and Generalized Parton Distributions,” *Phys. Rev. Lett.* **115** (21), 212003, [arXiv:1504.02009 \[hep-ex\]](#).
- Jung, Ju-Hyun, Ulugbek Yakhshiev, and Hyun-Chul Kim (2014a), “Energy–momentum tensor form factors of the nucleon within a soliton model,” *J. Phys. G* **41**, 055107, [arXiv:1310.8064 \[hep-ph\]](#).
- Jung, Ju-Hyun, Ulugbek Yakhshiev, Hyun-Chul Kim, and Peter Schweitzer (2014b), “In-medium modified energy-momentum tensor form factors of the nucleon within the framework of a π - ρ - ω soliton model,” *Phys. Rev. D* **89** (11), 114021, [arXiv:1402.0161 \[hep-ph\]](#).
- Kharzeev, D (1996), “Quarkonium interactions in QCD,” *Proc. Int. Sch. Phys. Fermi* **130**, 105–131, [arXiv:nucl-th/9601029](#).
- Kharzeev, Dmitri E (2021), “Mass radius of the proton,” *Phys. Rev. D* **104** (5), 054015, [arXiv:2102.00110 \[hep-ph\]](#).
- Kim, Hyun-Chul, Peter Schweitzer, and Ulugbek Yakhshiev (2012), “Energy-momentum tensor form factors of the nucleon in nuclear matter,” *Phys. Lett. B* **718**, 625–631, [arXiv:1205.5228 \[hep-ph\]](#).
- Kim, June-Young, and Hyun-Chul Kim (2021), “Energy-momentum tensor of the nucleon on the light front: Abel tomography case,” *Phys. Rev. D* **104** (7), 074019, [arXiv:2105.10279 \[hep-ph\]](#).
- Kim, June-Young, Hyun-Chul Kim, Maxim V. Polyakov, and Hyeon-Dong Son (2021), “Strong force fields and stabilities of the nucleon and singly heavy baryon Σ_c ,” *Phys. Rev. D* **103** (1), 014015, [arXiv:2008.06652 \[hep-ph\]](#).
- Kim, June-Young, and Bao-Dong Sun (2021), “Gravitational form factors of a baryon with spin-3/2,” *Eur. Phys. J. C* **81** (1), 85, [arXiv:2011.00292 \[hep-ph\]](#).
- Kim, June-Young, Bao-Dong Sun, Dongyan Fu, and Hyun-Chul Kim (2022a), “Mechanical structure of a spin-1 particle,” [arXiv:2208.01240 \[hep-ph\]](#).
- Kim, June-Young, Ulugbek Yakhshiev, and Hyun-Chul Kim (2022b), “Medium modification of the nucleon mechanical properties: Abel tomography case,” *Eur. Phys. J. C* **82** (8), 719, [arXiv:2204.10093 \[hep-ph\]](#).
- Kivel, N, Maxim V. Polyakov, and M. Vanderhaeghen (2001), “DVCS on the nucleon: Study of the twist - three effects,” *Phys. Rev. D* **63**, 114014, [arXiv:hep-ph/0012136](#).
- Kobzarev, I Yu, and L. B. Okun (1962), “Gravitational interaction of fermions,” *Zh. Eksp. Teor. Fiz.* **43**, 1904–1909.
- Kopeliovich, B Z, Ivan Schmidt, and M. Siddikov (2010), “DDVCS on nucleons and nuclei,” *Phys. Rev. D* **82**, 014017, [arXiv:1005.4621 \[hep-ph\]](#).
- Kou, Wei, Rong Wang, and Xurong Chen (2021), “Determination of the Gluonic D-term and Mechanical Radii of Proton from Experimental data,” [arXiv:2104.12962 \[hep-ph\]](#).
- Krutov, A F, and V. E. Troitsky (2021), “Pion gravitational form factors in a relativistic theory of composite particles,” *Phys. Rev. D* **103** (1), 014029, [arXiv:2010.11640 \[hep-ph\]](#).
- Krutov, A F, and V. E. Troitsky (2022), “Relativistic composite-particle theory of the gravitational form factors of the pion: Quantitative results,” *Phys. Rev. D* **106** (5), 054013, [arXiv:2201.04991 \[hep-ph\]](#).
- Kubis, Bastian, and Ulf-G. Meissner (2000), “Virtual photons in the pion form-factors and the energy momentum tensor,” *Nucl. Phys. A* **671**, 332–356, [Erratum: *Nucl.Phys.A* 692, 647–648 (2001)], [arXiv:hep-ph/9908261](#).
- Kumano, S, Qin-Tao Song, and O. V. Teryaev (2018), “Hadron tomography by generalized distribution amplitudes in pion-pair production process $\gamma^*\gamma \rightarrow \pi^0\pi^0$ and gravitational form factors for pion,” *Phys. Rev. D* **97** (1), 014020, [arXiv:1711.08088 \[hep-ph\]](#).
- Kumar, Narinder, Chandan Mondal, and Neetika Sharma (2017), “Gravitational form factors and angular momentum densities in light-front quark-diquark model,” *Eur. Phys. J. A* **53** (12), 237, [arXiv:1712.02110 \[hep-ph\]](#).
- Kumericki, Kresimir, Simonetta Liuti, and Herve Moutarde (2016), “GPD phenomenology and DVCS fitting: Entering the high-precision era,” *Eur. Phys. J. A* **52** (6), 157, [arXiv:1602.02763 \[hep-ph\]](#).
- Kumerički, Krešimir (2019), “Measurability of pressure inside the proton,” *Nature* **570** (7759), E1–E2.
- Laue, M (1911), “Zur Dynamik der Relativitätstheorie,” *Annalen Phys.* **340** (8), 524–542.
- von Laue, Max (1911), “Zur Dynamik der Relativitätstheorie,” *Annalen Phys.* **35**, 524.
- Leader, E, and C. Lorcé (2014), “The angular momentum controversy: What’s it all about and does it matter?” *Phys. Rept.* **541** (3), 163–248, [arXiv:1309.4235 \[hep-ph\]](#).
- Leutwyler, H, and Mikhail A. Shifman (1989), “Goldstone bosons generate peculiar conformal anomalies,” *Phys. Lett. B* **221**, 384–388.
- Lin, Huey-Wen (2021), “Nucleon Tomography and Generalized Parton Distribution at Physical Pion Mass from Lattice QCD,” *Phys. Rev. Lett.* **127** (18), 182001, [arXiv:2008.12474 \[hep-ph\]](#).
- Liuti, S, and S. K. Taneja (2005), “Nuclear medium modifications of hadrons from generalized parton distributions,” *Phys. Rev. C* **72**, 034902, [arXiv:hep-ph/0504027](#).
- Lorcé, Cédric (2013a), “Geometrical approach to the proton spin decomposition,” *Phys. Rev. D* **87** (3), 034031, [arXiv:1205.6483 \[hep-ph\]](#).
- Lorcé, Cédric (2013b), “Wilson lines and orbital angular momentum,” *Phys. Lett. B* **719**, 185–190, [arXiv:1210.2581 \[hep-ph\]](#).
- Lorcé, Cédric (2018a), “On the hadron mass decomposition,” *Eur. Phys. J. C* **78** (2), 120, [arXiv:1706.05853 \[hep-ph\]](#).
- Lorcé, Cédric (2018b), “The relativistic center of mass in field theory with spin,” *Eur. Phys. J. C* **78** (9), 785, [arXiv:1805.05284 \[hep-ph\]](#).
- Lorcé, Cédric (2020), “Charge Distributions of Moving Nucleons,” *Phys. Rev. Lett.* **125** (23), 232002, [arXiv:2007.05318 \[hep-ph\]](#).
- Lorcé, Cédric (2021), “Relativistic spin sum rules and the role of the pivot,” *Eur. Phys. J. C* **81** (5), 413, [arXiv:2103.10100 \[hep-ph\]](#).
- Lorcé, Cédric, and Peter Lowdon (2020), “Universality of the

- Poincaré gravitational form factor constraints,” *Eur. Phys. J. C* **80** (3), 207, arXiv:1908.02567 [hep-th].
- Lorcé, Cédric, Luca Mantovani, and Barbara Pasquini (2018), “Spatial distribution of angular momentum inside the nucleon,” *Phys. Lett. B* **776**, 38–47, arXiv:1704.08557 [hep-ph].
- Lorcé, Cédric, Andreas Metz, Barbara Pasquini, and Simone Rodini (2021), “Energy-momentum tensor in QCD: nucleon mass decomposition and mechanical equilibrium,” *JHEP* **11**, 121, arXiv:2109.11785 [hep-ph].
- Lorcé, Cédric, Hervé Moutarde, and Arkadiusz P. Trawiński (2019), “Revisiting the mechanical properties of the nucleon,” *Eur. Phys. J. C* **79** (1), 89, arXiv:1810.09837 [hep-ph].
- Lorcé, Cédric, Bernard Pire, and Qin-Tao Song (2022a), “Kinematical higher-twist corrections in $\gamma^*\gamma \rightarrow M\bar{M}$,” arXiv:2209.11140 [hep-ph].
- Lorcé, Cédric, Peter Schweitzer, and Kemal Tezgin (2022b), “2D energy-momentum tensor distributions of nucleon in a large- N_c quark model from ultrarelativistic to nonrelativistic limit,” *Phys. Rev. D* **106** (1), 014012, arXiv:2202.01192 [hep-ph].
- Lowdon, Peter, Kelly Yu-Ju Chiu, and Stanley J. Brodsky (2017), “Rigorous constraints on the matrix elements of the energy-momentum tensor,” *Phys. Lett. B* **774**, 1–6, arXiv:1707.06313 [hep-th].
- Ma, Yan-Qing, and Jian-Wei Qiu (2018), “Exploring Partonic Structure of Hadrons Using ab initio Lattice QCD Calculations,” *Phys. Rev. Lett.* **120** (2), 022003, arXiv:1709.03018 [hep-ph].
- Mai, Manuel, and Peter Schweitzer (2012a), “Energy momentum tensor, stability, and the D-term of Q-balls,” *Phys. Rev. D* **86**, 076001, arXiv:1206.2632 [hep-ph].
- Mai, Manuel, and Peter Schweitzer (2012b), “Radial excitations of Q-balls, and their D-term,” *Phys. Rev. D* **86**, 096002, arXiv:1206.2930 [hep-ph].
- Mamo, Kiminad A, and Ismail Zahed (2020), “Diffractive photoproduction of J/ψ and Υ using holographic QCD: gravitational form factors and GPD of gluons in the proton,” *Phys. Rev. D* **101** (8), 086003, arXiv:1910.04707 [hep-ph].
- Mamo, Kiminad A, and Ismail Zahed (2021), “Nucleon mass radii and distribution: Holographic QCD, Lattice QCD and GlueX data,” *Phys. Rev. D* **103** (9), 094010, arXiv:2103.03186 [hep-ph].
- Mamo, Kiminad A, and Ismail Zahed (2022), “ J/ψ near threshold in holographic QCD: A and D gravitational form factors,” *Phys. Rev. D* **106** (8), 086004, arXiv:2204.08857 [hep-ph].
- Masuda, M, et al. (Belle) (2016), “Study of π^0 pair production in single-tag two-photon collisions,” *Phys. Rev. D* **93** (3), 032003, arXiv:1508.06757 [hep-ex].
- McAllister, R W, and R. Hofstadter (1956), “Elastic Scattering of 188-MeV Electrons From the Proton and the α Particle,” *Phys. Rev.* **102**, 851–856.
- Mecking, B A, et al. (CLAS) (2003), “The CEBAF Large Acceptance Spectrometer (CLAS),” *Nucl. Instrum. Meth. A* **503**, 513–553.
- Metz, Andreas, Barbara Pasquini, and Simone Rodini (2020), “Revisiting the proton mass decomposition,” *Phys. Rev. D* **102**, 114042, arXiv:2006.11171 [hep-ph].
- Metz, Andreas, Barbara Pasquini, and Simone Rodini (2021), “The gravitational form factor $D(t)$ of the electron,” *Phys. Lett. B* **820**, 136501, arXiv:2104.04207 [hep-ph].
- Mondal, Chandan (2016), “Longitudinal momentum densities in transverse plane for nucleons,” *Eur. Phys. J. C* **76** (2), 74, arXiv:1511.01736 [hep-ph].
- Mondal, Chandan, Narinder Kumar, Harleen Dahiya, and Dipankar Chakrabarti (2016), “Charge and longitudinal momentum distributions in transverse coordinate space,” *Phys. Rev. D* **94** (7), 074028, arXiv:1608.01095 [hep-ph].
- More, Jai, Asmita Mukherjee, Sreeraj Nair, and Sudeep Saha (2022), “Gravitational form factors and mechanical properties of a quark at one loop in light-front Hamiltonian QCD,” *Phys. Rev. D* **105** (5), 056017, arXiv:2112.06550 [hep-ph].
- Müller, Dieter, Tobias Lautenschlager, Kornelija Passek-Kumericki, and Andreas Schaefer (2014), “Towards a fitting procedure to deeply virtual meson production - the next-to-leading order case,” *Nucl. Phys. B* **884**, 438–546, arXiv:1310.5394 [hep-ph].
- Müller, Dieter, D. Robaschik, B. Geyer, F. M. Dittes, and J. Hořejši (1994), “Wave functions, evolution equations and evolution kernels from light ray operators of QCD,” *Fortsch. Phys.* **42**, 101–141, arXiv:hep-ph/9812448.
- Nambu, Yoichiro, and G. Jona-Lasinio (1961a), “Dynamical Model of Elementary Particles Based on an Analogy with Superconductivity. I.” *Phys. Rev.* **122**, 345–358.
- Nambu, Yoichiro, and G. Jona-Lasinio (1961b), “Dynamical Model of Elementary Particles Based on an Analogy with Superconductivity. II,” *Phys. Rev.* **124**, 246–254.
- Neubelt, Matt J, Andrew Sampino, Jonathan Hudson, Kemal Tezgin, and Peter Schweitzer (2020), “Energy momentum tensor and the D-term in the bag model,” *Phys. Rev. D* **101** (3), 034013, arXiv:1911.08906 [hep-ph].
- Nielsen, N K (1977), “The Energy Momentum Tensor in a Nonabelian Quark Gluon Theory,” *Nucl. Phys. B* **120**, 212–220.
- Novikov, V A, and Mikhail A. Shifman (1981), “Comment on the $\psi' \rightarrow J/\psi \pi \pi$ Decay,” *Z. Phys. C* **8**, 43.
- Ossmann, J, M. V. Polyakov, P. Schweitzer, D. Urbano, and K. Goetze (2005), “The Generalized parton distribution function $(E^u + E^d)(x, \xi, t)$ of the nucleon in the chiral quark soliton model,” *Phys. Rev. D* **71**, 034011, arXiv:hep-ph/0411172.
- Owa, Shiryo, A. W. Thomas, and X. G. Wang (2022), “Effect of the pion field on the distributions of pressure and shear in the proton,” *Phys. Lett. B* **829**, 137136, arXiv:2106.00929 [hep-ph].
- Özdem, U, and K. Azizi (2020), “Gravitational form factors of hyperons in light-cone QCD,” *Phys. Rev. D* **101** (11), 114026, arXiv:2003.12588 [hep-ph].
- Pagels, Heinz (1966), “Energy-Momentum Structure Form Factors of Particles,” *Phys. Rev.* **144**, 1250–1260.
- Panteleeva, Julia Yu, and Maxim V. Polyakov (2020), “Quadrupole pressure and shear forces inside baryons in the large N_c limit,” *Phys. Lett. B* **809**, 135707, arXiv:2004.02912 [hep-ph].
- Panteleeva, Julia Yu, and Maxim V. Polyakov (2021), “Forces inside the nucleon on the light front from 3D Breit frame force distributions: Abel tomography case,” *Phys. Rev. D* **104** (1), 014008, arXiv:2102.10902 [hep-ph].
- Pasquini, B, and S. Boffi (2007), “Nucleon spin densities in a light-front constituent quark model,” *Phys. Lett. B* **653**, 23–28, arXiv:0705.4345 [hep-ph].
- Pasquini, B, M. V. Polyakov, and M. Vanderhaeghen (2014), “Dispersive evaluation of the D-term form factor in deeply virtual Compton scattering,” *Phys. Lett. B* **739**, 133–138,

- arXiv:1407.5960 [hep-ph].
- Pedrak, A, B. Pire, L. Szymanowski, and J. Wagner (2020), “Electroproduction of a large invariant mass photon pair,” *Phys. Rev. D* **101** (11), 114027, arXiv:2003.03263 [hep-ph].
- Pefkou, Dimitra A, Daniel C. Hackett, and Phiala E. Shanahan (2021), “Gluon gravitational structure of hadrons of different spin,” arXiv:2107.10368 [hep-lat].
- Perevalova, I A, M. V. Polyakov, and P. Schweitzer (2016), “On LHCb pentaquarks as a baryon- $\psi(2S)$ bound state: prediction of isospin- $\frac{3}{2}$ pentaquarks with hidden charm,” *Phys. Rev. D* **94** (5), 054024, arXiv:1607.07008 [hep-ph].
- Petrov, V Yu, P. V. Pobylitsa, Maxim V. Polyakov, I. Bornig, K. Goeke, and C. Weiss (1998), “Off - forward quark distributions of the nucleon in the large N_c limit,” *Phys. Rev. D* **57**, 4325–4333, arXiv:hep-ph/9710270.
- Pire, B, L. Szymanowski, and J. Wagner (2011), “NLO corrections to timelike, spacelike and double deeply virtual Compton scattering,” *Phys. Rev. D* **83**, 034009, arXiv:1101.0555 [hep-ph].
- Pisano, S, et al. (CLAS) (2015), “Single and double spin asymmetries for deeply virtual Compton scattering measured with CLAS and a longitudinally polarized proton target,” *Phys. Rev. D* **91** (5), 052014, arXiv:1501.07052 [hep-ex].
- Politzer, H David (1973), “Reliable Perturbative Results for Strong Interactions?” *Phys. Rev. Lett.* **30**, 1346–1349, [274(1973)].
- Polyakov, Maxim V (2003), “Generalized parton distributions and strong forces inside nucleons and nuclei,” *Phys. Lett. B* **555**, 57–62, arXiv:hep-ph/0210165.
- Polyakov, Maxim V, and Peter Schweitzer (2018a), “D-term, strong forces in the nucleon, and their applications,” arXiv:1801.05858 [hep-ph].
- Polyakov, Maxim V, and Peter Schweitzer (2018b), “Forces inside hadrons: pressure, surface tension, mechanical radius, and all that,” *Int. J. Mod. Phys. A* **33** (26), 1830025, arXiv:1805.06596 [hep-ph].
- Polyakov, Maxim V, and Hyeon-Dong Son (2018), “Nucleon gravitational form factors from instantons: forces between quark and gluon subsystems,” *JHEP* **09**, 156, arXiv:1808.00155 [hep-ph].
- Polyakov, Maxim V, and Bao-Dong Sun (2019), “Gravitational form factors of a spin one particle,” *Phys. Rev. D* **100** (3), 036003, arXiv:1903.02738 [hep-ph].
- Polyakov, Maxim V, and C. Weiss (1999), “Skewed and double distributions in pion and nucleon,” *Phys. Rev. D* **60**, 114017, arXiv:hep-ph/9902451.
- Prakash, Madappa, James M. Lattimer, Jose A. Pons, Andrew W. Steiner, and Sanjay Reddy (2001), “Evolution of a neutron star from its birth to old age,” *Lect. Notes Phys.* **578**, 364–423, arXiv:astro-ph/0012136.
- Qiu, Jian-Wei, and Zhite Yu (2022), “Exclusive production of a pair of high transverse momentum photons in pion-nucleon collisions for extracting generalized parton distributions,” *JHEP* **08**, 103, arXiv:2205.07846 [hep-ph].
- Radyushkin, A V (1996), “Scaling limit of deeply virtual Compton scattering,” *Phys. Lett. B* **380**, 417–425, arXiv:hep-ph/9604317.
- Radyushkin, A V (2017), “Quasi-parton distribution functions, momentum distributions, and pseudo-parton distribution functions,” *Phys. Rev. D* **96** (3), 034025, arXiv:1705.01488 [hep-ph].
- Raya, Khepani, Zhu-Fang Cui, Lei Chang, Jose-Manuel Morgado, Craig D. Roberts, and Jose Rodriguez-Quintero (2022), “Revealing pion and kaon structure via generalised parton distributions,” *Chin. Phys. C* **46** (1), 013105, arXiv:2109.11686 [hep-ph].
- Rodini, S, A. Metz, and B. Pasquini (2020), “Mass sum rules of the electron in quantum electrodynamics,” *JHEP* **09**, 067, arXiv:2004.03704 [hep-ph].
- Rutherford, E (1919), “Collision of α particles with light atoms. IV. An anomalous effect in nitrogen,” *Phil. Mag. Ser. 6* **37**, 581–587.
- Sachs, R G (1962), “High-Energy Behavior of Nucleon Electromagnetic Form Factors,” *Phys. Rev.* **126**, 2256–2260.
- Schweitzer, P, S. Boffi, and M. Radici (2002), “Polynomiality of unpolarized off forward distribution functions and the D term in the chiral quark soliton model,” *Phys. Rev. D* **66**, 114004, arXiv:hep-ph/0207230.
- Seder, E, et al. (CLAS) (2015), “Longitudinal target-spin asymmetries for deeply virtual Compton scattering,” *Phys. Rev. Lett.* **114** (3), 032001, [Addendum: *Phys.Rev.Lett.* **114**, 089901 (2015)], arXiv:1410.6615 [hep-ex].
- Shanahan, P E, and W. Detmold (2019a), “Gluon gravitational form factors of the nucleon and the pion from lattice QCD,” *Phys. Rev. D* **99** (1), 014511, arXiv:1810.04626 [hep-lat].
- Shanahan, P E, and W. Detmold (2019b), “Pressure Distribution and Shear Forces inside the Proton,” *Phys. Rev. Lett.* **122** (7), 072003, arXiv:1810.07589 [nucl-th].
- Shifman, Mikhail A, A. I. Vainshtein, and Valentin I. Zakharov (1978), “Remarks on Higgs Boson Interactions with Nucleons,” *Phys. Lett. B* **78**, 443–446.
- Snow, G A, and M. M. M. M. Shapiro (1961), “Mesons and Hyperons,” *Rev. Mod. Phys.* **33**, 231–231.
- Stepanyan, S, et al. (CLAS) (2001), “Observation of exclusive deeply virtual Compton scattering in polarized electron beam asymmetry measurements,” *Phys. Rev. Lett.* **87**, 182002, arXiv:hep-ex/0107043.
- Sun, Bao-Dong, and Yu-Bing Dong (2020), “Gravitational form factors of ρ meson with a light-cone constituent quark model,” *Phys. Rev. D* **101** (9), 096008, arXiv:2002.02648 [hep-ph].
- Sun, Peng, Xuan-Bo Tong, and Feng Yuan (2021), “Perturbative QCD analysis of near threshold heavy quarkonium photoproduction at large momentum transfer,” *Phys. Lett. B* **822**, 136655, arXiv:2103.12047 [hep-ph].
- Tanaka, Kazuhiro (2018), “Operator relations for gravitational form factors of a spin-0 hadron,” *Phys. Rev. D* **98** (3), 034009, arXiv:1806.10591 [hep-ph].
- Tanaka, Kazuhiro (2019), “Three-loop formula for quark and gluon contributions to the QCD trace anomaly,” *JHEP* **01**, 120, arXiv:1811.07879 [hep-ph].
- Tanaka, Kazuhiro (2022), “Twist-four gravitational form factor at NNLO QCD from trace anomaly constraints,” arXiv:2212.09417 [hep-ph].
- Teryaev, O V (1999), “Spin structure of nucleon and equivalence principle,” arXiv:hep-ph/9904376.
- Teryaev, O V (2001), “Crossing and radon tomography for generalized parton distributions,” *Phys. Lett. B* **510**, 125–132, arXiv:hep-ph/0102303.
- Tong, Xuan-Bo, Jian-Ping Ma, and Feng Yuan (2021), “Gluon gravitational form factors at large momentum transfer,” *Phys. Lett. B* **823**, 136751, arXiv:2101.02395 [hep-ph].
- Tong, Xuan-Bo, Jian-Ping Ma, and Feng Yuan (2022), “Perturbative Calculations of Gravitational Form Factors at Large Momentum Transfer,” arXiv:2203.13493 [hep-ph].

- Vanderhaeghen, M, Pierre A. M. Guichon, and M. Guidal (1999), “Deeply virtual electroproduction of photons and mesons on the nucleon: Leading order amplitudes and power corrections,” *Phys. Rev. D* **60**, 094017, [arXiv:hep-ph/9905372](#).
- Varma, Mira, and Peter Schweitzer (2020), “Effects of long-range forces on the D-term and the energy-momentum structure,” *Phys. Rev. D* **102** (1), 014047, [arXiv:2006.06602 \[hep-ph\]](#).
- Voloshin, M B, and A. D. Dolgov (1982), “On gravitational interaction of the Goldstone bosons,” *Sov. J. Nucl. Phys.* **35**, 120–121.
- Voloshin, Mikhail B, and Valentin I. Zakharov (1980), “Measuring QCD Anomalies in Hadronic Transitions Between Onium States,” *Phys. Rev. Lett.* **45**, 688.
- Wakamatsu, M (2007), “On the D-term of the nucleon generalized parton distributions,” *Phys. Lett. B* **648**, 181–185, [arXiv:hep-ph/0701057](#).
- Wakamatsu, Masashi (2014), “Is gauge-invariant complete decomposition of the nucleon spin possible?” *Int. J. Mod. Phys. A* **29**, 1430012, [arXiv:1402.4193 \[hep-ph\]](#).
- Wang, Gen, Yi-Bo Yang, Jian Liang, Terrence Draper, and Keh-Fei Liu (chiQCD) (2021), “Proton momentum and angular momentum decompositions with overlap fermions,” [arXiv:2111.09329 \[hep-lat\]](#).
- Wang, Xiao-Yun, Fancong Zeng, and Quanjin Wang (2022), “Gluon gravitational form factors and mechanical properties of proton,” [arXiv:2208.03186 \[hep-ph\]](#).
- Witten, Edward (1979), “Baryons in the $1/N$ Expansion,” *Nucl. Phys. B* **160**, 57–115.
- Won, Ho-Yeon, June-Young Kim, and Hyun-Chul Kim (2022), “Gravitational form factors of the baryon octet with flavor SU(3) symmetry breaking,” [arXiv:2210.03320 \[hep-ph\]](#).
- Workman, R L, et al. (Particle Data Group) (2022a), “Review of Particle Physics,” *PTEP* **2022**, 083C01.
- Workman, R L, et al. (Particle Data Group) (2022b), “Review of Particle Physics,” *PTEP* **2022**, 083C01.
- Yang, Yi-Bo, Ming Gong, Jian Liang, Huey-Wen Lin, Keh-Fei Liu, Dimitra Pefkou, and Phiala Shanahan (2018a), “Nonperturbatively renormalized glue momentum fraction at the physical pion mass from lattice QCD,” *Phys. Rev. D* **98** (7), 074506, [arXiv:1805.00531 \[hep-lat\]](#).
- Yang, Yi-Bo, Jian Liang, Yu-Jiang Bi, Ying Chen, Terrence Draper, Keh-Fei Liu, and Zhaofeng Liu (2018b), “Proton Mass Decomposition from the QCD Energy Momentum Tensor,” *Phys. Rev. Lett.* **121** (21), 212001, [arXiv:1808.08677 \[hep-lat\]](#).
- Yang, Yi-Bo, Raza Sabbir Sufian, Andrei Alexandru, Terrence Draper, Michael J. Glatzmaier, Keh-Fei Liu, and Yong Zhao (2017), “Glue Spin and Helicity in the Proton from Lattice QCD,” *Phys. Rev. Lett.* **118** (10), 102001, [arXiv:1609.05937 \[hep-ph\]](#).
- Zweig, G (1964), “An SU(3) model for strong interaction symmetry and its breaking. Version 1,” .